Nonlinear Optical Response of the Exciton-Excitonic Molecule System

by

Tetuji Tokihiro

Contents

Chapter 1 Introduction

Nonlinear optical properties of solids are being studied extensively. Remarkable progress in laser spectroscopic techniques has made possible the detailed microscopic studies of nonlinear optical processes. These studies give us possibilities of potential applications to optoelectronic and optical devices.

The effect of giant oscillator strength associated with excitation of excitonic molecules enhances extremely the nonlinear optical processes under two-photon resonance of the excitonic molecules.[1] Giant two-photon absorption, two-photon Raman scattering and luminescence due to the excitonic molecule have been investigated in detail experimentally as well as theoretically.[2-5] Here the two-photon Raman scattering is four-photon process in which two photons excite the excitonic molecule and one-photon is emitted leaving behind an exciton polariton in solids. When we increase the excitation power, we observe higher order nonlinear optical phenomena, e.g., shifts of Raman lines and new lines in the Raman scattering spectrum.[6-9] These new lines are analized in the first half of this thesis from the microscopic point of view. This affords us profound comprehension about various important properties such as the competition between coherent and incoherent processes, the transient behaviors and so on. Origins of these new lines can be classified into coherent and incoherent higher order optical processes.[10]

In the second half of the present thesis, we discuss another striking nonlinear optical phenomenon of optical bistability due to this exciton-excitonic molecule system. It brings about not

only a good example to understand nonequilibrium statistical physics, but also has the possibilities for applications to valuable device on the basis of the hysteresis and differential gain shown in its optical input-output characteristics. This optical device is being considered to be used as essential parts of an optical integrated circuit as well as an optical computer, in which light plays the role of electron in large scale integrated circuit in modern electronic computer.[11,12)]

This bistable behaviour results from the combined effect of the nonlinear optical response of the medium and the feed-back provided by Fabry-Perot resonator to the beam, and was observed in semiconductor etalons such as GaAs and InSb.[13,14)] Gibbs et al. used the nonlinear dispersive response due to the really excited elementary excitations. So that their switch-off time is governed by the longitudinal relaxation time of the excitations and is rather long ($\sim 10^{-8}$sec). This is one of the largest obstacle to get a more effective device than very large scale integrated circuit of Si or Josephson junctions.

An optical bistable system using the coherent optical nonlinearity induced by the giant oscillator strength in semiconductors, especially in CuCl, has been proposed.[15)] This system was shown to have the possibility of responding in an order of pico-second, which will remove that crucial obstacle to application to the more effective optical device. Several attempts have been devoted to the theoretical study of this system.[16-18)] Some recent preliminary experimental results in CuCl have demonstrated the existence of optical bistability, which, however, do not coincide numerically with any one of these

theoretical works.[19,20] The holding power is more than 10^2 times higher than expected in Refs.[15],[16], and the off-resonance condition required in Refs.[17],[18] is not satisfied. To clear up the cause of inconsistencies is very important for the sake of application to the optical device as well as understanding the microscopic details of optical bistability.

The present thesis is just devoted to the study of these subjects. In paticular, the following problems are intended to be clarified;

(1) What is the origin of the new emission bands under strong pumping?
(What determines their peculiar characteristics?)

(2) Why are the observed optical bistable responses inconsistent with the theoretical works?

(3) Can this optical device respond in an order of pico-second under rather low holding power as predicted before?

The key to these problems is the fact that there exists the competition between coherent processes and incoherent processes even in these nonlinear phenomena just as in the second order optical processes.

In the first half of this thesis, we consider the emission from highly excited crystal irradiated by monocromatic laser beam. The radiation field and the polarization field in the crystal interact with each other and form the hybridized waves, the quantum of which is called the polariton.[21] The emission processes can be understood microscopically as multi-polariton scattering, that is, many polaritons are scattered simultaneously through the real and virtual creation of excitonic molecules. We

formulate the emission spectrum of multi-polariton scattering by means of Green's function method, fully taking into account of really and virtually excited excitonic molecules. The perturbation expansions of this expression in terms of polariton amplitudes turn to be corresponding to the new Raman line and new emission bands mentioned above. Thus the first question is answered.

The second half of this thesis is devoted to the investigation of optical bistability in this polariton-excitonic molecule system. The stationary and transient behaviours are discussed in terms of nonlinear integral-difference equations. We show that this system represents two types of optical bistability; one is caused by coherent two-photon excitation and the other is caused by the real creation of excitonic molecules. It is considered that the latter process induced the optical bistability observed in CuCl. The second and third problems have been solved simultaneously. The optically bistable response due to this incoherent process can explain the experimental conditions. This is realized under near two-photon resonant excitation of the excitonic molecule and the higher holding power than the coherent process is required. Under this coherent excitation of the excitonic molecule it will be shown that the optical bistability is realized at a lower pump field and can be switched between the on- and the off-states in the order of 10 pico-second. The instability of this system is also discussed. Throughout this thesis, we shall know how the competition between coherent processes and incoherent processes are reflected in nonlinear optical phenomena.

Chapter 2 Multi-Polariton Scattering via Excitonic Molecules

§2-1 Introduction

In the course of optical processes, the system interacts with its environment.Under two-photon excitation in direct-band-gap semiconductors, we have two channels, i.e., a hyper-Raman scattering and a luminescence. The former is a coherent two-polariton scattering via virtual creation of an excitonic molecule and no exchange of energy takes place with the environment. On the other hand, the latter is an incoherent emission from a really excited excitonic molecule converted from two polaritons and an energy exchange with the environment is accompanied. The competitive behaviour between those two channels can be observed in emission spectra and has been studied in detail both experimentally and theoretically.[5,6)]

On the increase of the excitation power, higher order nonlinear emission processes are expected to become observable some of which are purely coherent and the others are incoherent or partially coherent. (Here, "coherent process" means that the scattered polaritons have a coherency with incident polaritons and, of cource, no energy exchange with its environment occurs.)

From a microscopical point of view, these processes can be described as coherent, incoherent or partially coherent multi-polariton scattering. For example, a process where four incident polaritons are scattered via two virtually excited excitonic molecules conserving their total energy and momentum is considered as a coherent four-polariton scattering. When a really excited excitonic molecule is dissociated into two polaritons and these polaritons interact with two incident polaritons, this

process is considered as an incoherent (partially coherent) four-polariton scattering.

In the next section, we derive the expression of the emission spectrum for multi-polariton scattering, which contains any order of coherent and incoherent processes.

§2-2 Emission Spectrum

The Hamiltonian of the polariton-excitonic molecule system under consideration is given as

$$\mathcal{H} = \mathcal{H}_0 + \nu \tag{2.1}$$

$$\mathcal{H}_0 = \sum_k \hbar\omega_p(k) A_k^\dagger A_k + \hbar\omega_m(k) B_k^\dagger B_k, \tag{2.2a}$$

$$\nu = \sum_{k,Q} -\hbar g(k,Q-k)(B_{-Q}-B_Q^\dagger)(A_{Q-k}-A_{-Q+k}^\dagger)(A_k+A_{-k}^\dagger), \tag{2.2b}$$

where A_k and $A_k^\dagger$ (B_k and $B_k^\dagger$) are annihilation and creation operators of a polariton (an excitonic molecule) with momentum k and energy $\hbar\omega_p(k)$ ($\hbar\omega_m(k)$), $g(k,k')$ is a coupling constant of forming an excitonic molecule with k+k' from two polaritons with k and k' and contains the giant oscillator strength.

When the crystal is irradiated with a strong monocromatic laser field at a nearly two-photon resonance of an excitonic molecule, the polariton with this frequency ω_0 and wave vector k_0 and the virtual excitation of an excitonic moleucle with $2\omega_0$ and $2k_0$ are induced in the crystal.

This virtual excitation causes the hyper-Raman scattering and keeps the coherency of the polariton, so that its amplitude ($F_0 e^{-2i\omega_0 t}$) is related to that of the polariton ($E_0 e^{-i\omega_0 t}$) through the first order of the interaction as:

$$F_0 = g(k_0,k_0)E_0^2/[\omega_m(2k_0)-2\omega_0-i\gamma_m] \tag{2.3}$$

with a transverse relaxation constant γ_m of an excitonic molecule.

The really excited excitonic molecules are also formed on their dispersion $\omega_m(Q)$ at the same time through the interaction with the environment such as phonons, impurities and so on. They are decomposed into incoherent polaritons, which are observed as luminescent light. The amplitudes of these excitonic molecules $\{F'_Q\}$ are determined by taking account of effects associated with the relaxation processes.[22)]

With the macroscopic occupation of the incident polariton, the coherent excitonic molecule and the incoherent excitonic molecule as the initial state, coherent and incoherent excitations of the higher orders are formed through multi-polariton scatterings. In order to describe these situations, we use the coherent state description of the system with these excitations at $t=-\infty$;

$$|t\rangle_S \xrightarrow[t\to-\infty]{} D_p(E_0 e^{-i\omega_0 t}) D_m(F_0 e^{-2i\omega_0 t}, \{F'_Q e^{-i\omega_m(Q)t}\}) \times |0\rangle_p |0\rangle_m , \tag{2.4}$$

where, $|t\rangle_s$ is the state vector, $|0\rangle_p$ and $|0\rangle_m$ are the vacuum states of polariton and excitonic molecule, respectively, and D_p (D_m) is the Glauber unitary displacement operator for polariton (excitonic molecule):[23)]

$$D_p(E_k(t)) = \exp[E_k(t)A_k^\dagger - E_k^*(t)A_k], \tag{2.5}$$

$$D_m(\{F_Q(t)\}) = \sum_Q \exp[F_Q(t)B_Q^\dagger - F_Q^*(t)B_Q]. \tag{2.6}$$

Then, we perform the time dependent canonical transformation:

$$|t\rangle_S \equiv D_p(E_0 e^{-i\omega_0 t}) D_m(\cdots)\ |t\rangle. \tag{2.7}$$

According to this transformation, the initial state and the Hamiltonian are converted into

$$|t> \xrightarrow[t \to -\infty]{} |0>_p |0>_m \ , \tag{2.8}$$

$$H(t) = H_0 + V_1(t) + V_2^{coh}(t) + V_2^{inc}(t) + V_3 \ , \tag{2.9}$$

$$H_0 = \sum_{\mathbf{k}} [\hbar\omega_p(\mathbf{k}) A_{\mathbf{k}}^\dagger A_{\mathbf{k}} + \hbar\omega_m(\mathbf{k}) B_{\mathbf{k}}^\dagger B_{\mathbf{k}}] \ , \tag{2.10a}$$

$$V_1(t) = \sum_{\mathbf{k}} 2\hbar g(\mathbf{k},\mathbf{k}_0)(E_0 e^{-i\omega_0 t} B_{\mathbf{k}+\mathbf{k}_0}^\dagger A_{\mathbf{k}} + \text{h.c.}) \ , \tag{2.10b}$$

$$V_2^{coh}(t) = \sum_{\mathbf{k}} \hbar g(\mathbf{k},2\mathbf{k}_0-\mathbf{k})(F_0 e^{-2i\omega_0 t} A_{\mathbf{k}}^\dagger A_{2\mathbf{k}_0-\mathbf{k}}^\dagger + \text{h.c.}) \ , \tag{2.10c}$$

$$V_2^{inc}(t) = \sum_{\mathbf{Q}} \sum_{\mathbf{k}} \hbar g(\mathbf{k},\mathbf{Q}-\mathbf{k})(F'_{\mathbf{Q}} e^{-i\omega_m(\mathbf{Q})t} A_{\mathbf{k}}^\dagger A_{\mathbf{Q}-\mathbf{k}}^\dagger + \text{h.c.}) \ , \tag{2.10d}$$

$$V_3 = \sum_{\mathbf{Q}} \sum_{\mathbf{k}} \hbar g(\mathbf{k},\mathbf{Q}-\mathbf{k})(B_{\mathbf{Q}} A_{\mathbf{k}}^\dagger A_{\mathbf{Q}-\mathbf{k}}^\dagger + \text{h.c.}) \ . \tag{2.10e}$$

Here, we used the rotating wave approximation.

The formation rate of the polariton k is written as

$$W_{\mathbf{k}} = \lim_{t\to\infty} \frac{d}{dt} <t|A_{\mathbf{k}}^\dagger A_{\mathbf{k}}|t>. \tag{2.11}$$

The emission spectrum is given by $W_{\mathbf{k}}$ times the transmitting probability of the polariton at the surface, which is considered to be almost constant in the frequency region under consideration. Therefore we may consider $W_{\mathbf{k}}$ approximately as the emission spectrum.

We should notice that the interactions are arranged in the order of their magnitude;

$$V_1 > V_2^{coh} \gtrsim V_2^{inc} >> V_3.$$

So at first, we eliminate the time dependence of V_1 and V_2^{coh} under transformation into the rotating frame and diagonalize

H_0+V_1 under the unitary transformation:

$$\begin{pmatrix} \alpha_k \\ \beta_k \end{pmatrix} = \begin{pmatrix} C_{\alpha k}, & C_{\beta k} \\ -C_{\beta k}, & C_{\alpha k} \end{pmatrix} \begin{pmatrix} A_k \\ B_{k+k_0} \end{pmatrix}, \tag{2.12}$$

into the following form:

$$H_0+V_1 \Rightarrow \sum_k \hbar\omega_\alpha(k)\alpha_k^\dagger\alpha_k + \hbar\omega_\beta(k)\beta_k^\dagger\beta_k. \tag{2.13}$$

Here

$$2\omega_{\alpha,\beta}(k) = (\Delta_{pk}+\Delta_{mk+k_0}) \pm [(\Delta_{pk}-\Delta_{mk+k_0})^2+4|g_k|^2]^{1/2}$$

and

$$\begin{pmatrix} C_{\alpha k} \\ C_{\beta k} \end{pmatrix} = \begin{pmatrix} \Delta_{mk+k_0}-\omega_{\alpha k} \\ -g_k \end{pmatrix} \cdot [(\Delta_{mk+k_0}-\omega_{\alpha k})^2+|g_k|^2]^{-1/2}, \tag{2.14}$$

with $\Delta_p(k)=\omega_p(k)-\omega_0$, $\Delta_m(Q)=\omega_m(Q)-2\omega_0$ and $g_k=g(k,k_0)E_0$. Accordingly, we may rewrite W_k as follows:

$$W_k = 2\mathrm{Im}\langle 0|T\{A_k^\dagger A_k V(0)S(\infty,-\infty)\}|0\rangle_L. \tag{2.15}$$

Here, T is the time ordering operator, V(t) is the interaction representation of $V\equiv V_2^{coh}+V_2^{inc}+V_3$, $S(\infty,-\infty)\equiv\exp\{-\frac{i}{\hbar}\int_{-\infty}^{\infty}\tilde{V}(\tau)d\tau\}$ and the subscript L means that we should pick up only linked diagrams.

This expression is correct also in the presence of perpendicular relaxation processes as long as $\omega_{\alpha(\beta)}(k)$ is replaced by $\omega_{\alpha(\beta)}(k)-i\gamma_{\alpha(\beta)}(k)$.

Next, we calculate the contributions of V_2^{coh} and V_2^{inc} to the infinite order by means of the diagrammatic method developed by Belyaev.[24)]

Finally, V_3 is taken into account by usual Green's function techniques. We show the procedures in Appendix A. In order to

get the precise expression of W_k, we must solve very complicated simultaneous integral equations as shown in Appendix A. This, even numerical evaluation, is very difficult to solve because of the complex k dependence of coupling constants.

In the next sections, we calculate eq.(2.15) by the perturbational methods. These results in the lower order terms are concluded to correspond with the nonlinear phenomena observed by experiments.

§2-3 Perturbational expansion of the emission spectrum

The lowest order contribution to eq.(2.15) is written as;

$$W_{\mathbf{k}}^{(0)} = W_{\mathbf{k}}^{(R)} + W_{\mathbf{k}}^{(L)} , \tag{2.16}$$

$$W_{\mathbf{k}}^{(R)} = 2\,\mathrm{Im}\left[\int_{-\infty}^{\infty} dt_1 \langle 0|T\{A_{\mathbf{k}}^{\dagger}A_{\mathbf{k}}\tilde{V}_2^{coh}(0-)\tilde{V}_2^{coh}(t_1)\}|0\rangle\right] , \tag{2.17a}$$

$$W_{\mathbf{k}}^{(L)} = 2\,\mathrm{Im}\left[\int_{-\infty}^{\infty} dt_1 \langle 0|T\{A_{\mathbf{k}}^{\dagger}A_{\mathbf{k}}\tilde{V}_2^{inc}(0-)\tilde{V}_2^{inc}(t_1)\}|0\rangle\right] . \tag{2.17b}$$

By the direct calculation, we obtain

$$W_{\mathbf{k}}^{(R)} = |F_0 \cdot g(\mathbf{k}, 2\mathbf{k}_0-\mathbf{k})|^2 \sum_{\substack{\mu,\nu \\ =\{\alpha,\beta\}}} |C_{\mu_{\mathbf{k}}} C_{\nu_{\mathbf{k}}}|^2 \delta(\omega_{\mu\mathbf{k}}+\omega_{\nu 2\mathbf{k}_0-\mathbf{k}}) \tag{2.18a}$$

$$W_{\mathbf{k}}^{(L)} = \sum_{\mathbf{Q}} |F_{\mathbf{Q}}' \cdot g(\mathbf{k}, \mathbf{Q}-\mathbf{k})|^2 \sum_{\substack{\mu,\nu \\ =\{\alpha,\beta\}}} |C_{\mu_{\mathbf{k}}} C_{\nu_{\mathbf{k}}}|^2 \delta(\omega_{\mu\mathbf{k}} + \omega_{\nu\mathbf{Q}-\mathbf{k}} - \Delta\omega_{\mathbf{Q}}) , \tag{2.18b}$$

where $\Delta\omega_{\mathbf{Q}} \equiv \omega_m(\mathbf{Q})-2\omega_0$.

As realized from the diagram of Fig.1-a which corresponds to $W_{\mathbf{k}}^{(R)}$, a coherent polarization due to an excitonic molecule at $2\mathbf{k}_0$ and $2\omega_0$ is converted into two polaritons, and one of these is observed as a Raman line. We have four ways for combinations of two renormalized polaritons α and β as shown in eq.(2.18a).

Thus, additional Raman lines are expected to be observed, depending on the frequency ω_0, intensity of the laser field E_0 and the direction of the wave vector k.

In §2-4, we reconsider these Raman scatterings on the basis of the dispersion anomaly, taking into account an infinite series of coherent excitation.

The diagrams of the next higher order processes are shown in Fig.2-a and Fig.2-b. The corresponding coherent terms in eq.(2.15) are;

$$\begin{aligned} W_{\mathbf{k}}^{(1;c)} &= 2\,\mathrm{Im}\Big[\int_{-\infty}^{\infty}\!\!\int\!\!\int dt_1 dt_2 dt_3 \langle 0|T\{A_{\mathbf{k}}^{\dagger}A_{\mathbf{k}}\tilde{V}_3(0-) \\ &\quad \times \tilde{V}_3(t_1)\tilde{V}_2^{coh}(t_2)\tilde{V}_2^{coh}(t_3)\}|0\rangle \\ &= |F_0\cdot g(\mathbf{k},2\mathbf{k}_0-\mathbf{k})|^2 \sum_{\mathbf{q}} |g(\mathbf{k},\mathbf{q})|^2 \sum_{\mu\nu\lambda} |C_{\mu\mathbf{k}}C_{\nu 2\mathbf{k}_0-\mathbf{k}-\mathbf{q}}C_{\lambda\mathbf{q}}|^2 \\ &\quad \times |G_{BA^+}(\mathbf{k}+\mathbf{q},-\omega_{\nu 2\mathbf{k}_0-\mathbf{k}-\mathbf{q}})|^2 \delta(\omega_{\mu\mathbf{k}}+\omega_{\lambda\mathbf{q}}+\omega_{\nu 2\mathbf{k}_0-\mathbf{k}-\mathbf{q}}) \ , \end{aligned} \tag{2.19a}$$

and

$$\begin{aligned} W_{\mathbf{k}}^{(2;c)} &= 2\,\mathrm{Im}\Big[\int_{-\infty}^{\infty}\cdots dt_1\cdots dt_5 \langle 0|T\{A_{\mathbf{k}}^{\dagger}A_{\mathbf{k}}\tilde{V}_3(0-)\tilde{V}_3(t_1) \\ &\quad V_2^{coh}(t_2)V_2^{coh}(t_3)V_2^{coh}(t_4)V_2^{coh}(t_5)\}|0\rangle\Big] \\ &= |F_0\cdot g(\mathbf{k},2\mathbf{k}_0-\mathbf{k})|^2 \sum_{\mathbf{q}_1\mathbf{q}_2} |g(\mathbf{k},\mathbf{q}_1)g(2\mathbf{k}_0-\mathbf{k}-\mathbf{q}_1+\mathbf{q}_2,\mathbf{q}_2)|^2 \\ &\quad \times \sum_{\substack{\mu_1,\mu_2 \\ \nu_1,\nu_2}} |C_{\mu_1\mathbf{k}}C_{\mu_1\mathbf{q}_1}C_{\nu_1\mathbf{q}_2}C_{\nu_2 2\mathbf{k}_0-\mathbf{k}-\mathbf{q}_1-\mathbf{q}_2}|^2 \\ &\quad \times |G_{BA^+}(\mathbf{k}+\mathbf{q}_1,\omega_{\nu_1\mathbf{q}_2}+\omega_{\nu_2 2\mathbf{k}_0-\mathbf{k}-\mathbf{q}_1-\mathbf{q}_2})|^2 \\ &\quad \times |G_{AB^+}(\mathbf{k}+\mathbf{q}_1,-\omega_{\nu_1\mathbf{q}_2}-\omega_{\nu_2 2\mathbf{k}_0-\mathbf{k}-\mathbf{q}_1-\mathbf{q}_2})|^2 \\ &\quad \times \delta(\omega_{\mu_1\mathbf{k}}+\omega_{\mu_2\mathbf{q}_1}+\omega_{\nu_1\mathbf{q}_2}+\omega_{\nu_2 2\mathbf{k}_0-\mathbf{k}-\mathbf{q}_1-\mathbf{q}_2}) \ , \end{aligned} \tag{2.19b}$$

where

$$|G_{BA+}(k,\omega)|^2 = |G_{AB+}(k,\omega)|^2$$
$$= |C_{\alpha k}C_{\beta k}|^2 \left| \frac{1}{\omega-\omega_{\alpha k}+i\gamma_\alpha} - \frac{1}{\omega-\omega_{\beta k}+i\gamma_\beta} \right|^2$$

Incoherent terms can be expressed in the same manner:

$$W_k^{(1;i)} = \sum_Q |F'_Q g(k,Q-k)|^2 \sum_q |g(k,q)|^2 \sum_{\mu\nu\lambda} |C_{\mu k}C_{\nu Q-k-q}C_{\lambda q}|^2$$
$$\times |G_{BA+}(k+q,-\omega_{\nu Q-k-q})|^2 \delta(\omega_{\mu k}+\omega_{\lambda q}+\omega_{\nu Q-k-q}-\Delta\omega_Q) \qquad (2.20a)$$

and

$$W_k^{(2;i)} = \sum_Q |F'_Q g(k,Q-k)|^2 \sum_{q_1 q_2} |g(k,q_1)g(Q-k-q_1-q_2,q_2)|^2$$
$$\times \sum_{\substack{\mu_1\mu_2 \\ \nu_1\nu_2}} |C_{\mu_1 k}C_{\mu_2 q_1-k}C_{\nu_1 q_2}C_{\nu_2 Q-q_1-q_2}|^2$$
$$\times |G_{BA+}(q_1,\omega_{\mu_2 q_1-k}+\omega_{\mu_1 k})|^2$$
$$\times |G_{AB+}(Q-q_1,\Delta\omega_Q-\omega_{\mu_1 k}-\omega_{\mu_2 q_1-k})|^2$$
$$\times \delta(\omega_{\mu_1 k}+\omega_{\mu_2 q_1-k}+\omega_{\nu_1 q_2}+\omega_{\nu_2 Q-q_1-q_2}) \qquad (2.20b)$$

As shown in Fig.2-a, $W_k^{(1;c)}$ is the rate at which two renormalized polaritons are formed from a coherent excitonic molecule and one of them is resolved into two renormalized polaritons.

A renormalized polariton is regarded as a composite particle of a polariton and an excitonic molecule, so that one of the most important processes contained in $W_k^{(1;c)}$ is the following one: Two polaritons created by a coherent excitonic molecule interact individually with incident polaritons and form two excitonic molecules. Then, one of them decomposes into two polaritons and

we observe one of these polaritons.

The corresponding term in eq.(2.19a) is written approximately as

$$\sum_{\mathbf{q}} \left| F_0 g(\mathbf{k}, 2\mathbf{k}_0 - \mathbf{k}) g(\mathbf{k}, \mathbf{q}) C_{\beta \mathbf{k}} C_{\beta\, 2\mathbf{k}_0 - \mathbf{k} - \mathbf{q}} C_{\alpha \mathbf{q}} C_{\alpha\, \mathbf{k}+\mathbf{q}} C_{\beta\, \mathbf{k}+\mathbf{q}} \right|^2$$

$$\times \frac{1}{\{\omega_m(4\mathbf{k}_0 - \mathbf{k} - \mathbf{q}) + \omega_m(\mathbf{k}+\mathbf{q}) - 4\omega_0\}^2 + \gamma_m^2}$$

$$\times \delta[\omega_m(4\mathbf{k}_0 - \mathbf{k} - \mathbf{q}) + \omega_p(\mathbf{k}) + \omega_p(\mathbf{q}) - 4\omega_0] \quad . \tag{2.21}$$

The emission spectrum due to this process is determined dominantly by the last two factors as the prefactors may be considered as constants. This process has a larger contribution only for $\omega_0 \geq \frac{1}{2}\omega_m(\mathbf{k}_0)$, as realized from the second factor of eq.(2.21).

On the other hand, almost all the contributions of the incoherent process $W_{\mathbf{k}}^{(1;i)}$ is to increase the intensity of luminescence.

In the next higher order processes shown in Fig.2-b, the main terms of the coherent process ($W_{\mathbf{k}}^{(2;c)}$) is only the slight correction to $W_{\mathbf{k}}^{(1;c)}$. But, $W_{\mathbf{k}}^{(2;i)}$ contains another emission process, that is, two polaritons formed from an incoherent excitonic molecule and two incident polaritons are scattered simultaneously into four polaritons through the virtual creation of two excitonic molecules.

The corresponding term in eq.(2.20b) is expressed approximately as

$$C \sum_{\mathbf{Q}\mathbf{q}} |F'_{\mathbf{Q}} C_{\alpha\mathbf{k}} C_{\alpha\mathbf{q}-\mathbf{k}}|^2 |C_{\alpha\mathbf{q}} C_{\beta\mathbf{q}} C_{\alpha\mathbf{Q}-\mathbf{q}} C_{\beta\mathbf{Q}-\mathbf{q}}|^2$$
$$\times [\{\omega_m(\mathbf{q}+\mathbf{k}_0)-\omega_p(\mathbf{q}-\mathbf{k}_0-\mathbf{k})-\omega_p(\mathbf{k})\}^2+\gamma_m^2]^{-1}$$
$$\times [\{2\omega_0+\omega_m(\mathbf{Q})-\omega_m(\mathbf{Q}-\mathbf{q}+\mathbf{k}_0)-\omega_p(\mathbf{q}+\mathbf{k}_0-\mathbf{k})-\omega_p(\mathbf{k})\}^2+\gamma_m^2]^{-1} , \quad (2.22)$$

where C is a constant derived from the summation over q_2, and we neglected its energy and wave vector dependence. $|C_{\alpha q} C_{\beta q}|^2$ and $|F_Q|^2$ have their maxima, respectively, around $q=k_0$ and at $Q=2k_0$. Therefore, the last two factors of eq.(2.22) are simplified into the following form neglecting some insignificant constants:

$$[\{\omega_m(2k_0)-\omega_p(2k_0-k)-\omega_p(k)\}^2+\gamma_m^2]^{-1}$$
$$\times[\{2\omega_0-\omega_p(2k_0-k)-\omega_p(k)\}^2+\gamma_m^2]^{-1}. \quad (2.23)$$

From this expression for a multiplication of the luminescence and the Raman spectra, we can realize that this process has an intermediate character between them. In fact for $|2\omega_0-\omega_m(2k)|<\gamma_m$, this emission spectrum has a single peak at $\omega_p(k)=\omega_0-\omega_p(2k_0-k)+\frac{1}{2}\omega_m(2k_0)$.

Contribution of much higher order optical processes can be calculated by the higher order expansion of $S(\infty,-\infty)$.

These processes may be observed as the shifts of Raman and luminescence lines or their asymmetric shapes. Really, the two-photon absorption spectra of excitonic molecules exhibit asymmetry under an intense excitaion,[4] which is considered to be partly caused by the higher-order multi-polariton effects.

§2-4 Bogolyubov transformation

Under the unitary transformation into rotating frame, $H_0+V_1(t)+$

$V_2^{coh}(t)$ is converted into a time-independent bilinear form, explicitly as:

$$H_0 + V_1(t) + V_2^{coh}(t) \longrightarrow \sum_{\mathbf{k}} H'_{\mathbf{k}} \tag{2.24}$$

$$\begin{aligned} H'_{\mathbf{k}} &= \Delta_p(\mathbf{k}) A^\dagger_{\mathbf{k}} A_{\mathbf{k}} + \Delta_m(\mathbf{k}+\mathbf{k}_0) B^\dagger_{\mathbf{k}+\mathbf{k}_0} B_{\mathbf{k}+\mathbf{k}_0} \\ &+ \Delta_p(2\mathbf{k}_0-\mathbf{k}) A^\dagger_{2\mathbf{k}_0-\mathbf{k}} A_{2\mathbf{k}_0-\mathbf{k}} + \Delta_m(3\mathbf{k}_0-\mathbf{k}) B^\dagger_{3\mathbf{k}_0-\mathbf{k}} B_{3\mathbf{k}_0-\mathbf{k}} \\ &+ g(\mathbf{k}_0,\mathbf{k}) E_0 B^\dagger_{\mathbf{k}+\mathbf{k}_0} A_{\mathbf{k}} + g(\mathbf{k}_0^*,\mathbf{k}) E_0^* B_{\mathbf{k}+\mathbf{k}_0} A^\dagger_{\mathbf{k}} \\ &+ g(\mathbf{k}_0,2\mathbf{k}_0-\mathbf{k}) E_0 B^\dagger_{3\mathbf{k}_0-\mathbf{k}} A_{2\mathbf{k}_0-\mathbf{k}} + g(\mathbf{k}_0^*,2\mathbf{k}_0-\mathbf{k}) E_0^* B_{3\mathbf{k}_0-\mathbf{k}} A^\dagger_{2\mathbf{k}_0-\mathbf{k}} \\ &+ g(\mathbf{k},2\mathbf{k}_0-\mathbf{k}) F_0 A^\dagger_{2\mathbf{k}_0-\mathbf{k}} A^\dagger_{\mathbf{k}} + g(\mathbf{k}^*,2\mathbf{k}_0-\mathbf{k}) F_0^* A_{2\mathbf{k}_0-\mathbf{k}} A_{\mathbf{k}} \ . \end{aligned} \tag{2.25}$$

We can easily diagonalize this Hamiltonian by means of Bogolyubov transformation.[25] This procedure is just the same as diagonalizing the photon-exciton Hamiltonian into the polariton Hamiltonian.[21] We define new annihilation and creation operators by the linear combinations of those of polariton and excitonic molecule:

$$\begin{pmatrix} \tilde{\alpha}_{\mathbf{k}} \\ \tilde{\beta}_{\mathbf{k}+\mathbf{k}_0} \\ \tilde{\alpha}_{2\mathbf{k}_0-\mathbf{k}} \\ \tilde{\beta}_{3\mathbf{k}_0-\mathbf{k}} \end{pmatrix} = \begin{pmatrix} C_{11} & C_{12} & C_{13} & C_{14} \\ C_{21} & C_{22} & C_{23} & C_{24} \\ C_{31} & C_{32} & C_{33} & C_{34} \\ C_{41} & C_{42} & C_{43} & C_{44} \end{pmatrix} \begin{pmatrix} A_{\mathbf{k}} \\ B_{\mathbf{k}+\mathbf{k}_0} \\ A_{2\mathbf{k}_0-\mathbf{k}} \\ B_{3\mathbf{k}_0-\mathbf{k}} \end{pmatrix} \tag{2.26}$$

Here, $\alpha_{\mathbf{k}}$ and $\beta_{\mathbf{k}}$ are normal-mode annihilation operators, thus they satisfy the following equations:

$$[\tilde{\alpha}_{\mathbf{k}} , H'_{\mathbf{k}}] = \hbar\omega_{\alpha\mathbf{k}} \tilde{\alpha}_{\mathbf{k}} ,$$

$$\text{and} \quad [\tilde{\beta}_{\mathbf{k}+\mathbf{k}_0} , H'_{\mathbf{k}}] = \hbar\omega_{\beta\mathbf{k}+\mathbf{k}_0} \tilde{\beta}_{\mathbf{k}+\mathbf{k}_0} , \tag{2.27}$$

and have the usual commutator relations

$$[C_{ik}\ ,\ C^{\dagger}_{jk'}] = \delta_{ij}\ \delta_{kk'}\ ,$$
$$[C_{ik}\ ,\ C_{jk'}] = [C^{\dagger}_{ik}\ ,\ C^{\dagger}_{jk'}] = 0 \quad (i,j=1,2), \tag{2.28}$$

where $C_{1k} \equiv \tilde{\alpha}_k$ and $C_{2k} \equiv \tilde{\beta}_k$. Using the Hamiltonian (2.25) and eq.(2.27), we get the normal-mode frequencies $\omega_{\alpha k}$ and $\omega_{\beta k}$ as the solution of the following eigenvalue problem:

$$\det \begin{Vmatrix} \Delta_p-\lambda, & g\ , & -f^*\ , & 0 \\ g^*\ , & \Delta_m-\lambda, & 0\ , & 0 \\ f\ , & 0\ , & -\Delta'_p-\lambda, & -g'^* \\ 0\ , & 0\ , & -g'\ , & -\Delta'_m-\lambda \end{Vmatrix} = 0\ , \tag{2.29}$$

where $\Delta_p \equiv \Delta_p(k)$, $\Delta_m \equiv \Delta_m(k+k_0)$, $\Delta'_p \equiv \Delta_p(2k_0-k)$, $\Delta'_m \equiv \Delta_m(3k_0-k)$, $g = g(k,k_0)\ E_0$, $g' \equiv g(k_0,2k_0-k)$, $f \equiv g(k,2k_0-k)F_0$. Equation (2.29) also gives the dispersion relation of renormalized polaritons, fully taking into account the coherent excitations. This dispersion relation is written as

$$E_i(k) = h(\lambda_i(k) + \omega_0) \quad (i=1,2,3,4), \tag{2.30}$$

where $\{\lambda_i\}$ are the eigenvalues determined by eq.(2.29), or, equivalently, the roots of an algebraic equation

$$\{(\lambda-\Delta_p)(\lambda-\Delta_m)-|g|^2\}\{(\lambda+\Delta'_p)(\lambda+\Delta'_m)-|g'|^2\}$$
$$+|f|^2(\lambda-\Delta_m)(\lambda+\Delta'_m)=0. \tag{2.31}$$

In the low intensity limit ($E_0 \to 0$), the eigen energies $\{E_i(k)\}$ reduce to $\{\hbar\omega_p(k),\ \hbar(\omega_m(k+k_0)-\omega_0),\ \hbar\omega_p(2k_0-k),\ \hbar(\omega_m(3k_0-k)-\omega_0)\}$. These eigen modes are regarded as the combined modes of ordinary polariton and induced polariton, i.e., the polarization induced by the transition from incident polariton to excitonic molecule.

As recognized from eq.(2.31), $\lambda_i(k)$ take complex values in some range of k. The modes which have complex eigen frequencies are unstable and either amplified or damped. When decreasing the excitation intensity ($|E_0|^2$), two of these amplified modes coincide with the modes of the scattered polaritons through the Raman scattering. Hence, these modes are considered to be corresponding to the polaritons formed by the coherent excitation and represent the shift of Raman line and new Raman lines. These are essentially the same lines observed and calculated by Grun et al..[8)]

It may be thought curious, however, that the eigenvalues of H_k take complex values in spite of its hermitian form shown in eq.(2.25), which describes a coherent two photon excitation:

$$V_{2k}^{coh} \equiv f\, A_k^\dagger A_{2k_0-k}^\dagger + f^* A_k A_{2k_0-k} \cdot$$

This interaction Hamiltonian is not a self-adjoints operator, so that the total Hamiltonian H_k becomes non-hermitian when the contribution of V_{2k}^{coh} exceeds that of other terms. (Here, "non-hermitian" means that the eigen vectors of this Hamiltonian do not belong to the Hilbert space.) This non-hermite Hamiltonian is essentially the same as that of the harmonic oscillator in the negative potential, i.e.,

$$H_{0S} = p^2 - \omega_0^2 x^2. \qquad (2.32)$$

In reality, we should add higher order terms such as $A_{k_1}^\dagger A_{k_2}^\dagger A_{k_3} A_{k_4}$, which are neglected in the present formulation, to H_k'. Then, the Hamiltonian retains its hermiticity, just as adding the fourth order term κx^4 to the non-hermite Hamiltonian

H_{0S}. The Hamiltonian H_k', therefore, is valid only when the amplitudes of these modes are small, and is considered to describe growing behaviour of these modes. The imaginary parts of its eigenvalues can be considered as the growing rates of them, as is noticed by setting up the equations of motion for them. In fact, as mentioned above, these complex modes are in accord with the polaritons scattered through the coherent excitation. Therefore, we discuss the nonlinear optical processes on the basis of this non-hermite Hamiltonian.

§2-5 Numerical results and discussion

In this section, we apply the results of the previous sections to the emission spectrum of CuCl.

The exciton in CuCl has a large oscillator strength and the excitonic molecule has a large binding energy (30meV) and stable at low temperature, so that nonlinear optical phenomena are enhanced under strong two-photon excitation.

Recently, Itoh et al. found new emission bands denoted by X- and L-bands.[9] The latter may correspond to the L-line reported previously without any assignment.[7] The characteristic features of these two emission lines are as follows;

(1) They are observed only under a strong excitation on the slightly higher energy side from the just two-photon resonance of an excitonic molecule. L_T and X_T lines are observed on the low frequency side of the Raman line M^R in which a transverse polariton is left in the crystal. On the other hand, L_L and X_L lines lie below another Raman line M_L with a longitudinal exciton left in the final states. Under

the just two-photon resonant excitation, their peak frequencies are coincident with those of M_T line and M_L line.

(2) The peak of L-bands are located just at midpoint between the two-photon Raman scattering and the luminescence lines. That is, the peak frequency shift is almost equal to the change of excitation frequency. On the other hand, the X-bands shift in the opposite sense.

(3) The peak energy and line shape of the X-bands do not depend on the scattering angle, while those of the L-bands do.

These features of X-bands and L-bands are well comformable to those of the emission processes $W^{(1;c)}$ and $W^{(2;i)}$, respectively, as discussed in Sect.2-3.

As for the X_L and L_L lines, we can repeat the similar calculations by adding the interaction term,

$$V_3' = \sum_{k,Q} \hbar g'(k,Q-k) B_Q^\dagger A_k A_{LQ-k} + h.c., \qquad (2.33)$$

where A_{Lk} is an annihilation operator of a longitudinal exciton with wave vector $\mathbf{k}$. The peak frequencies calculated from the expressions of these processes (eqs.(2.20),(2.21)) agree with the experimental results fairly well, as shown in Fig.3.

We conclude that two emission bands observed below M_T and M_L lines for $\omega_0 > \frac{1}{2}\omega_m(2k_0)$ under a strong excitation can be assigned to the four polariton scattering; X-bands and L-bands are corresponding to the scattering associated with the coherent excitation of excitonic molecules $(2\omega_0, 2k_0)$ and incoherently excited excitonic molecules $(\omega_m(2k_0), 2k_0)$, respectively. The ω_0 -dependence of these four lines can be perfectly explained by these processes as shown in Fig.3.

Only one discrepancy is the angular dependence of the splitting of two peaks in X_T-bands. Observed splitting is almost independent of k, i.e., the direction of observation, as the similar emission spectra were observed in the backward and the forward scattering. In this calculation, the splitting in the forward configuration is almost twice as large as the backward one as shown in Fig.3. This may be mainly due to the neglect of the relaxation and higher order effects. Really, the relaxation has an effect to reduce the difference between the backward and the forward scattering.

This discrepancy will be removed when the angular (k) dependence of X_T-bands is measured precisely and compared with those calculated taking into account both the effects of relaxation and higher order processes.

Chapter 3 Optical Bistability due to Excitonic Molecules

§3-1 Introduction

An optical bistable system is made to operate in two low- and high-transmitting states and this exhibits a hysteresis of transmitted power against change of incident power.[11,12] This optical bistability has been observed for the Fabry-Perot cavity of GaAs and InSb,[13,14] and the room-temperature operation is found to be possible in a GaAs-GaAlAs superlattice etalon.[26] These offered the possibility for all-optical devices as memories, logical operations, transistors etc.. It takes, however, 40-100 nano-second to switch off from the high to the low transmitted states. Gibbs et al. used the nonlinear response due to really excited elementary excitations, i.e., excitons in GaAs and electron-hole pairs in InSb. As a result, it takes a long decay time characteristic of these elementary excitations to switch-off.

In addition to this demerit, the energy of incident laser is partially dissipated into heat in these processes. This may prevent the high degree of accumulation of these optical devices.

On the other hand, the optical bistable system due to the coherent nonlinear polarization of an exciton-excitonic molecule system, which is the subject of the present paper, is considered to be free from these two disadvantages. This system was shown to be capable of being switched between the on- and off-states in the transverse relaxation time of the order of pico-second in some idealized situation, where the response of the medium is purely dispersive, so that the energy dissipation may be reduced very much.

Recently, Peyghambarian et al. observed optical limiting and bistable responses with 8 to 12 μm thick CuCl films sandwiched by 90 % reflecting mirrors.[12)]

The bistable behaviour was observed under nearly resonant two-photon excitations of the excitonic molecule with 7 to 14 MW/cm^2. The required holding power was 10^2 times the theoretically expected ones.[15,16)] This is inconsistent with the results by Sarid et al. and by Sung et al. that the optical bistability is possible only under an enough off-resonant condition.[17,18)]

In the present thesis, we formulate the dynamics of this system on the basis of a polariton picture, where the coherent coupling between incident photons and relevant excitons is fully taken into account. Here we can neglect the incoherently excited excitons under well off-resonant excitation from the exciton resonance. Then, the nonlinear optical response of the medium is caused by interactions of the polaritons with the two kinds of excitonic molecules, that is, coherent interaction of two polaritons through virtually excited excitonic molecules and incoherent interaction between the polariton and really created excitonic molecules. The stationary states show that, even under the nearly two-photon resonant excitation of excitonic molecule, two kinds of the optical bistability are possible due to the coherent nonlinear polarization at a low excitation power of the order of $0.1MW/cm^2$ and due to the incoherent one at a higher excitation power of the order of $10MW/cm^2$. The threshold power of the optical bistability depends in the opposite way on the off-resonant frequency of the two-photon transition to the excitonic molecule state. The coherent process is the same as in

Refs.[13],[14]. The incoherent process is quite different from the optical bistability observed in GaAs and InSb, but may correspond to that of CuCl observed by Peyghambarian et al., for this process is caused by the really created excitonic molecules, that is, it depends on the fifth order nonlinear optical susceptibility.

We also consider the effect due to a spatial oscillation of polariton fields which is neglected in the mean field theory. This effect comes out to be important when the sample length is of the same order of or shorter than the relevant wave length of the polariton.

We study the transient behaviour of system and show that the response time of the coherent optical bistability is determined primarily by that of the Fabry-Perot cavity, that is, the polariton decay time due to leakage from both ends.

Then the possibility of two beam optical bistability of this system and some instabilities are also discussed.

§3-2 Basic equations and boundary conditions

We consider a polariton-excitonic molecule system driven by the coherent laser field in a Fabry-Perot resonator with the length ℓ and reflectivity R at both ends. The Hamiltonian which describes the medium (polariton-excitonic molecule system) is,

$$H = \sum_{k}\omega_p(k)A_k A_k + \sum_{Q}\omega_m(Q)B_Q B_Q + \sum_{k,Q} G(k,Q-k)(A_k^\dagger A_{Q-k}^\dagger B_Q + \text{h.c.}), \tag{3.1}$$

where we take $\hbar=1$. This is represented in the momentum space.

On the other hand, the spatial representation of fields is inevitable to describe the boundary conditions at both ends. Here we introduce the following field operators:

$$\hat{\alpha}_F(\mathbf{r}) \equiv \sum_{k_Z>0} A_{\mathbf{k}} e^{i\mathbf{k}\cdot\mathbf{r}}, \qquad \hat{\alpha}_B(\mathbf{r}) \equiv \sum_{k_Z<0} A_{\mathbf{k}} e^{i\mathbf{k}\cdot\mathbf{r}}$$

$$\hat{\beta}_{F1}(\mathbf{r}) \equiv \sum_{Q_Z>k_Z>0} B_{\mathbf{Q}} A^{\dagger}_{\mathbf{Q}-\mathbf{k}} e^{i\mathbf{k}\cdot\mathbf{r}}, \qquad \hat{\beta}_{B1}(\mathbf{r}) \equiv \sum_{Q_Z<k_Z<0} B_{\mathbf{Q}} A^{\dagger}_{\mathbf{Q}-\mathbf{k}} e^{i\mathbf{k}\cdot\mathbf{r}}$$

$$\hat{\beta}_{F2}(\mathbf{r}) \equiv \sum_{\substack{Q_Z>k_Z \\ k_Z<0}} B_{\mathbf{Q}} A^{\dagger}_{\mathbf{Q}-\mathbf{k}} e^{i\mathbf{k}\cdot\mathbf{r}}, \qquad \hat{\beta}_{B2}(\mathbf{r}) \equiv \sum_{\substack{Q_Z<k_Z \\ 0<k_Z}} B_{\mathbf{Q}} A^{\dagger}_{\mathbf{Q}-\mathbf{k}} e^{i\mathbf{k}\cdot\mathbf{r}},$$

$$\hat{N}_F(\mathbf{r}) \equiv \sum_{\substack{Q_Z>\frac{k_0}{2} \\ \mathbf{Q}'}} B^{\dagger}_{\mathbf{Q}'} B_{\mathbf{Q}} e^{-i(\mathbf{Q}'-\mathbf{Q})\cdot\mathbf{r}},$$

$$\hat{N}_0(\mathbf{r}) \equiv \sum_{\substack{-\frac{k_0}{2}<Q_Z<\frac{k_0}{2} \\ \mathbf{Q}'}} B^{\dagger}_{\mathbf{Q}'} B_{\mathbf{Q}} e^{-i(\mathbf{Q}'-\mathbf{Q})\cdot\mathbf{r}},$$

$$\hat{N}_B(\mathbf{r}) \equiv \sum_{\substack{Q_Z<-\frac{k_0}{2} \\ \mathbf{Q}'}} B^{\dagger}_{\mathbf{Q}'} B_{\mathbf{Q}} e^{-i(\mathbf{Q}'-\mathbf{Q})\cdot\mathbf{r}}. \tag{3.2}$$

where k_0 is the wave vector of incident polariton propagating in the Z-direction, and $\{\hat{\alpha}(\mathbf{r})\}$, $\{\hat{\beta}(\mathbf{r})\}$ and $\{\hat{N}(\mathbf{r})\}$ are operators of normal polariton fields, nonlinear polariton fields and the populations of excitonic molecules, respectively. Physical meanings of these field operators are sketched in Fig.4. The equations of motion of these field operators are obtained by commuting these with Hamiltonian (3.1).

The next step is to determine the boundary conditions at the ends of the cavity. This is rather difficult because there exist not only normal polariton fields but also nonlinear polariton fields, i.e., this problem is a kind of the additional boundary

condition (A.B.C.).[27] This problem may be solved when we treat the coupling between the electromagnetic field and these excitations in the first principle, but, in our case, we can take an easier method.

The bistable operation is possible under the excitation of lower branch polariton. Under a weak excitaion, the single mode of polariton exists and the A.B.C. is unnecessary as far as the effect of the evanescent mode is neglected. The interaction between normal and nonlinear polaritons, however, is essential to give correct boundary conditions under the strong pumping, because the external field excites renormalized modes which are expressed approximately as a linear combination of normal and nonlinear polariton modes. As a result, we consider the A.B.C. here.

Now we write boundary conditions in the following forms:

$$\begin{aligned}
\alpha_F(0,\tau) &= tE_I'(\tau) + re^{i\delta}\alpha_B(0,\tau-2\Delta\tau), \\
\alpha_B(\Delta\tau,\tau) &= r\alpha_F(\Delta\tau,\tau) \\
\beta_{F1}(0,\tau) &= re^{i\delta}\beta_{B1}(0,\tau-2\Delta\tau) + t\, C_1E_I'(\tau), \\
\beta_{B1}(\Delta\tau,\tau) &= r\beta_{F1}(\Delta\tau,\tau), \\
\beta_{B2}(0,\tau) &= re^{-i\delta}\beta_{F2}(0,\tau-2\Delta\tau) + t\, C_2E_I'(\tau), \\
\beta_{F2}(\Delta\tau,\tau) &= r\beta_{B2}(\Delta\tau,\tau), \qquad (3.3)
\end{aligned}$$

where, $r=\sqrt{R}$, $t=\sqrt{1-R}$, δ is the detuning of Fabry-Perot cavity, and

$$\alpha_F(x,\tau) \equiv \langle\langle\hat{\alpha}_F(r)\rangle\rangle_t e^{i(\omega_0 t-k_0 Z)}$$

$$\alpha_B(x,\tau') \equiv \langle\langle\hat{\alpha}_B(r)\rangle\rangle_t e^{i\{\omega_0 t-k_0(2\ell-Z)\}}, \quad \text{etc..}$$

Here, $\langle\langle\cdots\rangle\rangle_t$ denotes a trace over the density matrix and an

average over horizontal sections, $\tau \equiv t - Z/v_g$, $\tau' \equiv t - (2\ell - Z)/v_g$, $x \equiv Z/v_g$ and $\Delta\tau \equiv \ell/v_g$, where v_g is the group velocity of normal polaritons which will be defined below. C_1 and C_2 are certain parameters dependent on inner variables such as $|\alpha_F(x,\tau)|^2$, and $E_I'(\tau)$ is a variable which is a function of the incident field and inner variables (see Appendix B). Note that these boundary conditions depend essentially on the strength of the normal polariton field. With these boundary conditions, we obtain difference-integral equations as follows,

$$
\begin{aligned}
&\alpha_F(x,\tau) - r^2 e^{i\delta}\alpha_F(x,\tau-2\Delta\tau) \\
&= tE_I'(\tau) - 2iG\int_0^x \beta_{F1}(\xi,\tau) + \beta_{F2}(\xi,\tau-2(\Delta\tau-\xi))\,d\xi \\
&\quad - 2iGr^2 e^{i\delta}\int_x^{\Delta\tau} \beta_{F1}(\xi,\tau-2\Delta\tau) + \beta_{F2}(\xi,\tau-2(\Delta\tau-\xi))\,d\xi \\
&\quad - 2iGre^{i\delta}\int_0^{\Delta\tau} \beta_{B1}(\xi,\tau-2\Delta\tau) + \beta_{B2}(\xi,\tau-2\xi)\,d\xi \ , \\
&\alpha_B(x,\tau) - r^2 e^{i\delta}\alpha_B(x,\tau-2\Delta\tau) \\
&= rtE_I'(\tau) - 2iGr\int_0^{\Delta\tau} \beta_{F1}(\xi,\tau) + \beta_{F2}(\xi,\tau-2(\Delta\tau-\xi))\,d\xi \\
&\quad - 2iGr^2 e^{i\delta}\int_0^x \beta_{B1}(\xi,\tau-2\Delta\tau) + \beta_{B2}(\xi,\tau-2\xi)\,d\xi \\
&\quad - 2iG\int_x^{\Delta\tau} \beta_{B1}(\xi,\tau) + \beta_{B2}(\xi,\tau-2\xi)\,d\xi \ , \\
&e^{i\tilde{\Delta}x}\beta_{F1}(x,\tau) - r^2 e^{i\delta - i\tilde{\Delta}(2\ell-x)}\beta_{F1}(x,\tau-2\Delta\tau) \\
&= rtC_1 e^{i\delta}E_I'(\tau) - iG\int_0^x d\xi\ e^{i\tilde{\Delta}\xi}\{|\alpha_F(\xi,\tau)|^2 - N_F(\xi,\tau)\}\alpha_F(\xi,\tau) \\
&\quad - iGr^2 e^{i\delta - 2i\tilde{\Delta}\ell}\int_x^{\Delta\tau} d\xi\ e^{i\tilde{\Delta}\xi}\{|\alpha_F(\xi,\tau-2\Delta\tau)|^2 - N_F(\xi,\tau-2\Delta\tau)\} \\
&\qquad \times \alpha_F(\xi,\tau-2\Delta\tau) \\
&\quad - iGre^{i\delta}\int_0^{\Delta\tau} d\xi\ e^{-i\tilde{\Delta}\xi}\{|\alpha_B(\xi,\tau-2\Delta\tau)|^2 - N_B(\xi,\tau-2\Delta\tau)\}\alpha_B(\xi,\tau-2\Delta\tau) \ ,
\end{aligned}
$$

$$e^{i\tilde{\Delta}(2\ell-x)}\beta_{B1}(x,\tau) - r^2 e^{i\delta-i\tilde{\Delta}x}\beta_{B1}(x,\tau-2\Delta\tau)$$

$$= r^2 tC_1 e^{i\delta}E_I'(\tau) - iGr\int_0^{\Delta\tau} d\xi\ e^{i\tilde{\Delta}\xi}\{|\alpha_F(\xi,\tau)|^2 - N_F(\xi,\tau)\}\alpha_F(\xi,\tau)$$

$$- iGr^2 e^{i\delta}\int_0^x d\xi\ e^{-i\tilde{\Delta}\xi}\{|\alpha_B(\xi,\tau-2\Delta\tau)|^2 - N_B(\xi,\tau-2\Delta\tau)\}\alpha_B(\xi,\tau-2\Delta\tau)$$

$$- iGe^{2i\tilde{\Delta}\ell}\int_x^{\Delta\tau} d\xi\ e^{-i\Delta\xi}\{|\alpha_B(\xi,\tau)|^2 - N_B(\xi,\tau)\}\alpha_B(\xi,\tau)\ ,$$

$$e^{i\tilde{\Delta}x}\beta_{B2}(x,\tau) - r^2 e^{-i\delta-2i\tilde{\Delta}\ell}e^{i\tilde{\Delta}x}\beta_{B2}(x,\tau-2\Delta\tau)$$

$$= tC_2E_I'(\tau) - iG\int_0^x d\xi\ e^{i\tilde{\Delta}\xi}\{|\alpha_F(\xi,\tau)|^2 - N_0^{(F)}(\xi,\tau)$$

$$- N_0^{(B)}(\xi,\tau-2(\Delta\tau-\xi))\}\alpha_B(\xi,\tau-2(\Delta\tau-\xi))$$

$$- iGr^2 e^{-i\delta-2i\tilde{\Delta}\ell}\int_x^{\Delta\tau} d\xi\ e^{i\tilde{\Delta}\xi}\{|\alpha_F(\xi,\tau-2\Delta\tau)|^2$$

$$- N_0^{(F)}(\xi,\tau-2\Delta\tau) - N_0^{(B)}(\xi,\tau-2(\Delta\tau-\xi))\}\alpha_B(\xi,\tau-2(2\Delta\tau-\xi))\ ,$$

$$e^{i\tilde{\Delta}(2\ell-x)}\beta_{F2}(x,\tau) - r^2 e^{-i\tilde{\Delta}x-i\delta}\beta_{F2}(x,\tau-2\Delta\tau)$$

$$= rtC_2E_I'(\tau) - iGr\int_0^{\Delta\tau} d\xi\ e^{i\tilde{\Delta}\xi}\{|\alpha_F(\xi,\tau)|^2 - N_0^{(F)}(\xi,\tau)$$

$$- N_0^{(B)}(\xi,\tau-2(\Delta\tau-\xi))\}\alpha_B(\xi,\tau-2(\Delta\tau-\xi))$$

$$- iGr^2 e^{-i\delta}\int_0^x d\xi\ e^{-i\tilde{\Delta}\xi}\{|\alpha_B(\xi,\tau-2\Delta\tau)|^2 - N_0^{(F)}(\xi,\tau-2\xi)$$

$$- N_0^{(B)}(\xi,\tau-2\Delta\tau)\}\alpha_F(\xi,\tau-2\xi)$$

$$- iGe^{2i\tilde{\Delta}\ell}\int_x^{\Delta\tau} d\xi\ e^{-i\tilde{\Delta}\xi}\{|\alpha_B(\xi,\tau)|^2 - N_0^{(B)}(\xi,\tau)$$

$$- N_0^{(F)}(\xi,\tau+2(\Delta\tau-\xi))\}\alpha_F(\xi,\tau+2(\Delta\tau-\xi))\ ,$$

$$
\begin{aligned}
&N_F(x,\tau) - e^{-\gamma\,\Delta\tau} N_F(x,\tau-\Delta\tau) \\
&= -iGe^{-\gamma\,\tau}\int_{\tau-\Delta\tau}^{\tau} d\eta\; e^{\gamma\,\eta}(\beta^*_{F1}(x,\eta)\alpha_F(x,\eta) - c.c.)\ , \\
&N_B(x,\tau) - e^{-\gamma\,\Delta\tau} N_B(x,\tau-\Delta\tau) \\
&= -iGe^{-\gamma\,\tau}\int_{\tau-\Delta\tau}^{\tau} d\eta\; e^{\gamma\,\eta}(\beta^*_{B1}(x,\eta)\alpha_B(x,\eta) - c.c.)\ , \\
&N_0^{(F)}(x,\tau) - e^{-\gamma\,\Delta\tau} N_0^{(F)}(x,\tau-\Delta\tau) \\
&= -iGe^{-\gamma\,\tau}\int_{\tau-\Delta\tau}^{\tau} d\eta\; e^{\gamma\,\eta}(\beta^*_{B2}(x,\eta)\alpha_F(x,\eta) - c.c.)\ , \\
&N_0^{(B)}(x,\tau) - e^{-\gamma\,\Delta\tau} N_0^{(B)}(x,\tau-\Gamma\tau) \\
&= -iGe^{-\gamma\,\tau}\int_{\tau-\Delta\tau}^{\tau} d\eta\; e^{\gamma\,\eta}(\beta^*_{F2}(x,\eta)\alpha_B(x,\eta) - c.c.)\ . \qquad (3.4)
\end{aligned}
$$

Here we used two approximations. First, we decoupled averages of multiplications of field operators, e.g., $\langle\langle\hat{\alpha}_F^\dagger(r)\hat{\alpha}_F(r)\hat{\alpha}_F(r)\rangle\rangle_t \longrightarrow |\alpha_F(x,t)|^2\alpha_F(x,t)$. This approximation is allowed when the system is coherently excited. Second, we made a slowly varying envelope approximation:

$$
\begin{aligned}
&\omega_p(k_0 - i\nabla_r) \simeq \omega_p(k_0) + \mathbf{v}_g\cdot(-i\nabla_r), \\
&G(k_0 - i\nabla_r, k_0 - i\nabla_r) \simeq G(k_0,k_0), \qquad (3.5)
\end{aligned}
$$

where $\mathbf{v}_g = (\frac{\partial\omega_p}{\partial\mathbf{k}})_{\mathbf{k}=\mathbf{k}_0}$ and $v_g = |\mathbf{v}_g|$. This is allowed when the temporal and spatial change of field operators is not so large, e.g., when

$$
\left|\frac{\partial^2}{\partial x^2}\,\alpha_F(x,\tau)\right| << \frac{1}{v_g}\left|\frac{\partial}{\partial x}\,\alpha_F(x,\tau)\right|\ . \qquad (3.6)
$$

Eqations (3.4) are basic equations in our analysis, and they are applicable so far as the approximations mentioned above are valid.

§3-3 Stationary solutions

We apply the equations derived in the previous section to the system of excitons and excitonic molecules in CuCl crystal.

In this section, we consider the stationary response. Expanding field operators into Fourier series,

$$\alpha_F(x) = \cdots + \alpha^{(-1)}e^{-i\Delta x} + \alpha^{(0)} + \alpha^{(1)}e^{i\Delta x} + \cdots$$

$$\beta_{Fl}(x) = \cdots + \beta^{(-1)}e^{-i\Delta x} + \beta^{(0)} + \beta^{(1)}e^{i\Delta x} + \cdots, \text{ etc.}, \tag{3.7}$$

we get nonlinear simultaneous equations of infinite order from eqs.(3.4). The K-th component $\alpha_F^{(K)}$ is at most of an order of $|G\alpha_F^{(0)}|^{2|K|}\alpha_F^{(0)}$, i.e.,

$$\alpha_F^{(K)} \leq O(|G\alpha_F^{(0)}|^{2|K|}\alpha_F^{(0)}) \tag{3.8}$$

and $|G\alpha_F^{(0)}|^2 \sim 1$ means the power of polariton field is over $50MW/cm^2$ in CuCl. In addition, for a large $|K|$ the fields show rapid changes in space and their spatial averages are small. Therefore it is sufficient to keep only terms to the order of $O(|G\alpha_F^{(0)}|^4\alpha_F^{(0)})$, that is, we take into consideration up to the fifth order susceptibility (χ_5). The result is

$$\begin{aligned}
&(1-r^2e^{i\delta})\alpha_F^{(0)} \\
&= tE_I' - 2iG(\frac{\ell}{2v_g})(1+r^2e^{i\delta})\beta_{Fl}^{(1)} - 2iG(\frac{1}{i\Delta})(1-r^2e^{i\delta-i\Delta'})\beta_{Fl}^{(0)} \\
&\quad - 2iG(\frac{\ell}{2v_g})(1+r^2e^{i\delta})\beta_{F2}^{(-1)} + 2iG(\frac{1}{i\Delta})(1-r^2e^{i\delta+i\Delta'})\beta_{F2}^{(0)} \\
&\quad - 2iGre^{i\delta}\{\frac{\ell}{v_g}\beta_{Bl}^{(-1)} + (\frac{e^{i\Delta'}-1}{i\Delta})\beta_{Bl}^{(0)} + \frac{\ell}{v_g}\beta_{B2}^{(1)} + (\frac{e^{-i\Delta'}-1}{-i\Delta})\beta_{B2}^{(0)}\}, \\
&\beta_{Fl}^{(1)} = -\frac{G}{\Delta}\{|\alpha_F^{(0)}|^2 - N_F^{(0)}\}\alpha_F^{(0)} \cdots,
\end{aligned} \tag{3.9}$$

where $\tilde{\Delta}=\Delta-i\Gamma$, $\Delta'=\tilde{\Delta}\cdot\ell/v_g$ and $\Delta\tau$ is replaced by $(\frac{\ell}{v_g})$ in order to make the system size dependence clear. The population of excitonic molecules is given as

$$N_F^{(0)} = \frac{2G}{\gamma_{\parallel}\cdot\ell}\{(\frac{1-e^{-\Gamma\ell}}{\tilde{\Delta}})\beta_{Fl}^{(0)}\alpha_F^{(0)*} + c.c.\}\cdots. \qquad (3.10)$$

But as shown in Ref.[4], the absorption spectra measured around the energy region of a giant two-photon absorption band are not Lorenzian, but obey an Urbach-Martienssen rule. Therefore, on the lower energy side, the population of incoherently created excitonic molecules decreases exponentially with increasing the off-resonant energy Δ.[28,29]

Furthermore the peak value of the population is rather different from the calculated value using eq.(3.10) for the high excitation power. These discrepancies are caused by the fact that, in the real system, there are many channels of creating excitonic molecules incoherently, such as impurity scattering, exciton-exciton collisions etc., but we have not evaluated these influences correctly, since they cannot be described by relaxation constants alone.

Therefore, it will be better to substitute experimental data $\{N^{(exp)}\}$ for $\{N^{(0)}\}$ in eqs.(3.9). $N_F^{(exp)}$ can be expressed according to the Ref.[4],

$$N_F^{(exp)} = \frac{A\cdot e^{-\Delta_m/(\gamma_{\parallel}+\gamma' I)}}{\gamma_{\parallel}+\gamma'\cdot I} I^2 , \qquad (3.11)$$

where A and γ' are constants given in Table 1 and $I=|\alpha_F^{(0)}|^2$. $N_0^{(exp)}$ and $N_B^{(exp)}$ have the similar expressions. Before showing the results of numerical calculation, we should comment about the deviation from the mean field theory. The forward propagating

polarization field $\alpha_F^{(0)}$ satisfies the following equation up to the third order nonlinear processes;

$$(1 - r^2 e^{i\delta})\alpha_F^{(0)} - tE_I'$$

$$= \frac{iG^2 \ell}{(\Delta - i\Gamma)v_g}(|\alpha_F^{(0)}|^2 + |\alpha_B^{(0)}|^2)\{(1+r^2 e^{i\delta})\alpha_F^{(0)} + 2re^{i\delta}\alpha_B^{(0)}\}$$

$$- \frac{2G}{(\Delta - i\Gamma)}\{(1-r^2 e^{i\delta - i\Delta'})\beta_{F1}^{(0)} - (1-r^2 e^{i\delta + i\Delta'})\beta_{F2}^{(0)}\}$$

$$+ \frac{2Gre^{i\delta}}{(\Delta - i\Gamma)}\{(1-e^{i\Delta'})\beta_{B1}^{(0)} - (1-e^{-i\Delta'})\beta_{B2}^{(0)}\} . \qquad (3.12)$$

In the mean field theory, only the first term on the right-hand side appears. The second and third terms describe the deviations from the mean field approximation. It is noted that the first term is proportional to the sample length, while the others are not. Accordingly, the deviation is negligible when the sample length ℓ is sufficiently large, but it comes out to be serious with reducing the length. In CuCl, the critical length is several microns, and, as mentioned below, coherent optical bistability can not occur when ℓ is shorter than 1.5 μm.

We performed numerical calculations with the material constants listed in Table 1. As expected, we have two types of optical bistability; one due to the coherent process and the other due to the incoherent one, depending upon the detuning and the incident power. The former is observed at the low incident power and the latter at the high incident power. The sample length and off-resonance dependence of their holding power are shown in Figs.5-10. We derive the characteristics of these two optical bistabilities in CuCl from them. First, the holding power required for the coherent optical bistability is by two

orders of magnitudes lower than that for the incoherent one. This is just the consequence of the fact that the coherent process is induced by χ_3 associated with coherent nonlinear polariton, whereas incoherent one is induced by χ_5 describing the real creation of excitonic molecules. Second, the ℓ dependence of the coherent optical bistability is opposite to that of incoherent one. This shows a competitive relation between these two processes. Third, the coherent optical bistability is realizable in the region $\ell \gtrsim 1.5\mu m$ and for the higher off-resonant energy, we need a smaller ℓ. This is caused by the combined effects of the negative contribution of χ_5 (incoherent process) and the deviation from the mean field theory, that is, the contribution of spatially oscillating components of the field operators.

Fourth, the coherent nonlinear polarization is approximately proportional to $\Delta/(\Delta^2+\Gamma^2)=(2\omega_0-\omega_m)/[\,(2\omega_0-\omega_m)^2+\Gamma^2]$. Therefore this is sensitive to the frequency fluctuation γ and the spectrum broadening of incident laser light. When the laser spectrum width $\Delta/2$ becomes of the same order as $\Delta/2$, contributions to coherent polarization cancel out each other. When the phase relxation Γ becomes larger than the fixed degree of the off-resonance Δ, the effect of coherent polarization is reduced.

Thus we may conclude that the optical bistability of CuCl etalon observed by Peyghambarian et al. and Levy et al. may be due to the incoherent process because the holding power is as large as 7 to 15 MW/cm^2 and it was observed only near the giant two-photon absorption of excitonic molecules. The holding power calculated here seems rather low compared with the experimental

data. This may be because our theory deals with very pure crystal irradiated by an absolutely coherent laser light, but in the actual situation crystal and laser light do not fulfill such a requirement.

To confirm this result, the otpical bistability should be observed under an sufficiently off-resonant excitaion ($\Delta >> \Gamma$) of the excitonic molecule by a laser light as coherent as possible and for CuCl crystal as pure as possible.

(It shoud be noted that we cannot have incoherent optical bistability if we do not replace $\{N\}$ by $\{N^{exp}\}$. Because, in the system with constant relaxation times, the contribution of incoherent processes cannot overcome that of coherent processes.)

§3-4 Transient response

In this section, we discuss the dynamics of this optical bistable system basing upon eqs.(3.4). As shown in the previous section, there exist two types of optical bistability, coherent and incoherent ones. The switching time of the former is dominated by the transverse relaxation time and the response time of the Fabry-Perot cavity. On the other hand, the latter responds in a rather long longitudinal relaxation time due to the real creation of excitonic molecules. The holding power required for an incoherent optical bistability is typically 100 times as high as that for the coherent optical bistability. Our interest lies, however, in the fast and low power switching process, therefore we mainly consider a coherent optical bistable response. (It is hard (if not impossible) to describe the time dependence of population of excitonic molecules, so that we replace $\{N\}$ by

$\{N^{(exp)}\}$. When we treat them with using effective longitudinal relaxation constants ($\gamma_{\parallel}$) and effective dipolemoment matrix element(G), the results are trivial, that is, the same as in the mean field theory using the constants determined by experiments.)

Coherent optical bistability is realizable at a low incident power, at which the contribution of χ_5 is negligible compared with χ_3. So we only retain terms up to $O(|G\alpha_F^{(0)}|^2\alpha_F^{(0)})$ in eqs.(3.4). We get

$$\begin{aligned}
&\alpha_F^{(0)}(\tau) - r^2 e^{i\delta}\alpha_F^{(0)}(\tau-2\Delta\tau) \\
&= tE_I'(\tau) - 2iG\left(\frac{\ell}{2v_g}\right)\{\beta_{F1}^{(1)}(\tau) + r^2 e^{i\delta}\beta_{F1}^{(1)}(\tau-2\Delta\tau)\} \\
&\quad - 2iG\left(\frac{1}{i\Delta'}\right)\{\beta_{F1}^{(0)}(\tau) - r^2 e^{i\delta - i\Delta'}\beta_{F1}^{(0)}(\tau-2\Delta\tau)\} \\
&\quad - 2iG\left(\frac{\ell}{2v_g}\right)(1+r^2 e^{i\delta})\beta_{F2}^{(-1)}(\tau-\Delta\tau) \\
&\quad - 2iG\left(\frac{-1}{i\Delta'}\right)(1-r^2 e^{i\delta+i\Delta'})\beta_{F2}^{(0)}(\tau-\Delta\tau) \\
&\quad - 2iGre^{i\delta}\{\left(\frac{\ell}{vg}\right)\beta_{B1}^{(-1)}(\tau-2\Delta\tau) + \left(\frac{e^{i\Delta'}-1}{i\Delta'}\right)\beta_{B1}^{(0)}(\tau-2\Delta\tau) \\
&\quad + \left(\frac{\ell}{v_g}\right)\beta_{B2}^{(1)}(\tau-\Delta\tau) + \left(\frac{e^{-i\Delta'}-1}{-i\Delta'}\right)\beta_{B2}^{(0)}(\tau-\Delta\tau)\} \ , \\
&\beta_{F1}^{(1)}(\tau) = -\frac{G}{\Delta'}|\alpha_F^{(0)}(\tau)|^2\alpha_F^{(0)}(\tau) \ , \cdots \ .
\end{aligned} \tag{3.13}$$

Here we approximate

$$\begin{aligned}
&\int_0^{\Delta\tau}\beta_{F2}(\xi,\tau-2(\Delta\tau-\xi))d\xi \simeq \int_0^{\Delta\tau}\beta_{F2}(\xi,\tau-\Delta\tau)d\xi \\
&\int_0^{\Delta\tau}\beta_{B2}(\xi,\tau-2\xi)d\xi \simeq \int_0^{\Delta\tau}\beta_{B2}(\xi,\tau-\Delta\tau)d\xi \ , \cdots \ .
\end{aligned} \tag{3.14}$$

This approximation is valid under the conditions

$$|\beta_{F2}(\xi,\tau)-\beta_{F2}(\xi,\tau-\Delta\tau)| << \Delta\tau|\beta_{F2}(\xi,\tau)|\cdots \ , \tag{3.15}$$

and these conditions are satisfied in our numerical calculations.

The switching behaviours of transmitted power with respect to the incident power are presented in Figs.11,12. We have computed the tansient responses varying several parameters such as the pulse width, intensity, shape and so on.

We list up the features of transient response we have observed. First, the shape of pulses does not affect so much the transient behaviours. Even in the case of a rectangular pulse, where this system suffers quite rapid change of the incident field, the amplitude of the transmitted field varies rather slowly as shown in Figs.11,12. This transient feature guarantees our asuumption of eqs.(3.14), (3.15).

Second, the larger the amplitude of the pulse comes to be, the shorter becomes the switching time. The shortening of the switching time is almost saturated when the pulse power exceeds the threshold by more than the hysteresis width. On the other hand, the system cannot be switched by the pulse exceeding the threshold power by less than half the hysteresis width.

Third, in the coherent optical bistability, both switch-off time and switch-on time are determined by the response time of Fabry-Perot cavity and given as:

$$t_s \simeq \frac{4\ell}{v_g(1-R)} \cdot \tag{3.16}$$

The numerical value of t_s is about 20 pico seconds for ℓ=2μm and R=0.9.

Since we fix the transverse relaxation time at Γ^{-1}=30 pico seconds and this is of the same order of the response time in the region of other material parameters with which we are concerned, we cannot deny that t_s is influenced by Γ. But, if the

transverse relaxation time is longer than the value we take, t_s will not change so much, because we consider an absolutely coherent process in space as well as in time, so that relaxation of the relevant mode is induced by multiplication of two types of phase modulation; one caused in the material (transverse relaxation) and the other due to the partial extinction of the mode at the surface (run-off from Fabry-Perot cavity). On the other hand, if it is much shorter, it is doubtful whether our assumption for spatial coherence is correct. In such a case, it may be more suitable to describe this system as an effective three level system interacting with laser field.[15)]

It is noted that any instability did not appear in the present numerical calculations in spite of rather complicated simultaneous nonlinear difference equations. From this fact, we may conclude that the coherent optical bistability in this system is stable against pulsation, chaos and so on.[30,31)] The response time of the cavity is much longer than the round trip time of the polariton because of high reflectivity of the mirrors at both ends. In addition to this, the holding power required in this system is relatively small. Thus, overshoot switching and the instabilities due to difference equations are suppressed. Furthermore we consider a good cavity limit, so that Lorentz chaos may not appear. We should mention that we have observed several chaotic behaviors of transmitted light in the incoherent optical bistability in the mean field theory with some values of material parameters. But we think they are intrinsic in the approximate difference equations and unphysical, for their temporal change is far beyond the efficiency of slowly varying

approximation and they seem to be suppressed by taking account of the spatially oscillating effects.

The switching time of incoherent optical bistability is dominated by the longitudinal relaxation time, i.e., the decay time of the population of really created excitonic molecules. It is rather short because of the giant-oscillator-strength effect in the radiative process. This makes the switch-off time of the incoherent optical bistability as short as 0.3 nano-seconds. The short switch-off time observed by Peyghambarian et al. is considered to be the result of this short longitudinal relaxation time of excitonic molecules.

§3-5 Concluding remarks

In this last section, we summarize our results and give some comments.

We have developed the theory of optical bistability from a microscopic point of view and applied it to the system of polariton-excitonic molecule in CuCl. We have found two types of optical bistability; coherent and incoherent ones. The former is the same type as proposed by Hanamura,[15] but the latter is a new type. The optical bistability observed by Peyghambarian et al. is considered to be this incoherent optical bistability.

The deviation from the mean field theory becomes crucial for the reduced system-length and off-resonant pumping. This is due to spatially oscillating effects of polarization fields.

Switching time of coherent optical bistability is as short as the response time of Fabry-Perot cavity, while that of incoherent one is dominated by the longitudinal relaxation time

of really populated excitonic molecules.

In addition, the holding power required in coherent optical bistability is almost 10^{-2} times as low as that in incoherent one, and no heat is produced in absolutely coherent process. Thus we think CuCl etalon is favorable for an optical bistable device by taking advantage of its coherent optical bistability. As for instabilities, we have not observed any instability in the course of numerical calculations for the coherent optical bistability. We conclude that so far as coherent optical bistability is concerned, this system will not represent instabilities such as Ikeda instability, overshoot switching and so on.

Now we discuss about the possibility of two beam optical bistability which is characteristic of the polariton-excitonic molecule system (three level system).

When this system is irradiated by a driving laser beam ($E_0 e^{i(\omega_0 t - \mathbf{k}_0 r)}$) and a probe beam ($E_1 e^{i(\omega_1 t - \mathbf{k}_1 r)}$), the reflectivity n and detuning ϕ is written as

$$n = n_0 + n'(\omega_0)I_0 + n''(\omega_1)I_1 \ , \tag{3.18a}$$

$$\phi = \phi_0 + \phi' \cdot I_0 + \phi'' \cdot I_1 \ , \tag{3.18b}$$

where $I_0=|E_0|^2$, $I_1=|E_1|^2$, n'(n") and $\phi'(\phi")$ are the coefficients of nonlinear reflectivity and detuning with respect to the driving (probe) field.

We consider the following situation;

$$\omega_0 + \omega_1 \simeq \omega_m(\mathbf{k}_0+\mathbf{k}_1),\ I_0 >> I_1 \text{ and } |\phi''| >> |\phi_0 + \phi' I_0| . \tag{3.19}$$

Then we notice $n'', \phi'' \propto (\omega_m - \omega_0 - \omega_1)^{-1}$. This situation is very

different from those we have considered so far, for the system can be switched not only with the change in the power but with that in the frequency of probe beam. The switching power is much lower than the one-beam optical bistability. The power required for switching (ΔI_2), compared with the one beam case (ΔI_1), is roughly estimated as:

$$\frac{\Delta I_2}{\Delta I_1} \sim \frac{1}{1+F\phi_0^2}\left|\frac{\omega_m(\mathbf{k}_0+\mathbf{k}_1)-\omega_0-\omega_1}{\omega_m(\mathbf{k}_0+\mathbf{k}_1)-2\omega_0}\right| , \tag{3.20}$$

where F is the finess of the Fabry-Perot cavity. An optical bistability of the probe beam is also possible. This optical bistability needs a low holding power and a low switching power, for the nonlinearity is enhanced by the strong driven field. The ratio of the holding power of the prove beam in this system (I_p) to that in one beam case (I_1) is given after some calculations as:

$$\frac{I_p}{I_1} \simeq \frac{1}{1+DI_1} , \tag{3.21}$$

where

$$D = \left|\frac{C^2(1+R)|G|^2}{2\pi(\omega_p-\omega_m)(\omega_m-\omega_0-\omega_1)}\right| .$$

These specific features are characteristic to the optical bistable system induced by the nonlinearity due to a two-photon transition.

Chapter 4 Summary

The nonlinear optical phenomena in polariton-excitonic molecule system, especially in CuCl, have been investigated theoretically. We have paid attention to the competitive behaviors of coherent and incoherent processes.

In the first part of this thesis, we studied the emission spectrum of this system under the strong incident fields. We have formulated its expression microscopically which does not have a conventional form such as the formula in soft X-ray problem.[32] The higher order emission processes can be understood as multi-polariton scatterings. Renormalization of the polariton dispersion, additional hyper-Raman scattering near two-photon resonance and new emission lines (X-lines, L-lines) could be explained systematically in this picture. We found X-lines are caused by purely coherent processes, while L-lines are induced from coherent and incoherent processes.

In the second part, we considered optical bistability of this system using the same Hamiltonian as used in the first part. We introduced field operators, derived equations of motion for them, and gave adequate boundary conditions. Two types of optical bistability were found to be realizable: one is due to coherent process and the other is due to incoherent process. These correspond to the two dominant processes discussed in the emission spectrum. The coherent optical bistability has a potential use for bistable device for the following three advantages; (1) low holding power, (2) fast switching and (3) small heat production. The optical bistable behaviours observed by Peyghambarian et al. in CuCl, however, are considerd due to

the incoherent process.

What are lacking to realize the coherent optical bistable response? First, we need a sample of CuCl so pure as the Urbach tail is observed at the two-photon absorption spectrum. Otherwise, the coherent polarization of the excitonic molecule may be smeared out in the background of the two-photon absorption due to the excitonic molecule associated with the phase relaxations due to scattering by impurities or defects.

Secondly, a coherent laser will be required to pump the coherent nonlinear polarization. Otherwise, destructive interference will kill the coherent nonlinear polarization under the multi-mode pumping.

We have demonstrated the disadvantage of the reduction in the thickness of the nonlinear optical medium from the calculation beyond the mean field theory. There the spatially oscillating fields reduced the nonlinear optical polarization effectively. We have not found an Ikeda instability, pulsation, chaos and so on in the present system. This optical bistable system under the coherent nonlinear optical process seems to be very stable as discussed in Sect.3-3.

Acknowledgments

The author wishes to express his sincere thanks to Professor E. Hanamura for suggesting the problems of the nonlinear optical phenomena, stimulating discussions and critical reading of a manuscript, and to Professor Y. Tanabe and Professor T. Fujiwara for kind instruction and continuous encouragement. He also thanks to Professor T. Itoh and Dr. K. Ohtaka for fruitful discussions about multi-polariton scattering, and Dr. M. Kuwata for helpful comments about CuCl crystal. This manuscript was typed by Miss T. Tokanai. Her fine work is gratefully acknowledged. Lastly the author would like to thank all the members of Rikigaku Kyoshitsu for their hospitality given to him.

§ Appendix A

In this appendix, the procedure for the calculation of the emission rate W_k in Sect.2-2 is briefly shown on the basis of the Green's function method.

We define the following Green's functions:

$$G_{A^\dagger A}(k,k';t) \equiv -i\langle 0|T\{A_k^\dagger(t)A_{k'},S_2(\infty)\}|0\rangle,$$

$$G_{A^\dagger B}(k,k';t) \equiv -i\langle 0|T\{A_k^\dagger(t)B_{k'+k_0}S_2(\infty)\}|0\rangle,$$

$$G_{B^\dagger A}(k,k';t) \equiv -i\langle 0|T\{B_{k+k_0}^\dagger(t)A_{k'},S_2(\infty)\}|0\rangle,$$

and $$G_{B^\dagger B}(k,k';t) \equiv -i\langle 0|T\{B_{k+k_0}^\dagger(t)B_{k'+k_0}S_2(\infty)\}|0\rangle, \qquad (A.1)$$

where $S_2(\infty) = \exp\{-i\int_{-\infty}^{\infty}d\tau[V_2^{coh}(\tau)+V_2^{inc}(\tau)]\}$

and we take the unit $\hbar=1$.

As shown in the diagrams of Fig.A-1, the Green's function $G_{A^\dagger A}(k,k';t)$ satisfies the following Dyson equations

$$G_{A^\dagger A}(k,k';t) = G_{A^\dagger A}^{(0)}(k;t)\cdot\delta_{kk'} + \sum_Q\int_{-\infty}^{\infty}d\tau\ f(k,Q;\tau) \times G_{A^\dagger A}^{(0)}(k;\tau)\check{G}_{A^\dagger A}(Q-k,k';t-\tau)$$

or,

$$= G_{A^\dagger A}^{(0)}(k;t)\delta_{k,k'} + \sum_Q\int_{-\infty}^{\infty}d\tau\ f^*(k',Q;\tau) \times\hat{G}_{A^\dagger A}(k,Q-k';\tau)\times G_{A^\dagger A}^{(0)}(k';t-\tau) \qquad (A.2)$$

where

$$G_{A^\dagger A}^{(0)}(k;t) \equiv -i\langle 0|T\{A^\dagger(t)A\}|0\rangle\ ,$$

$$f(k,Q;t) \equiv g(k,Q-k)\{F_0\delta_{Q,2k_0} + F_Q'e^{i\Delta_m(Q)t}\}\ ,$$

$$\check{G}_{A^\dagger A}(k,k';t) = \sum_Q\int_{-\infty}^{\infty}d\tau\ f^*(k,Q;\tau)G_{A^\dagger A}^{(0)}(k,-\tau)G_{A^\dagger A}(Q-k,k';t-\tau)\ , \qquad (A.3a)$$

and

$$\hat{G}_{A\dagger A}(\mathbf{k},\mathbf{k}';t) = \sum_{\mathbf{Q}}\int_{-\infty}^{\infty} d\tau\ f(\mathbf{k}',\mathbf{Q};\tau)G_{A\dagger A}(\mathbf{k},\mathbf{Q}-\mathbf{k}';\tau)G^{(0)}_{A\dagger A}(\mathbf{k}';\tau-t)\ . \tag{A.3b}$$

The other Green's functions are given as

$$G_{A\dagger B}(\mathbf{k},\mathbf{k}';t) = \sum_{\mathbf{Q}}\int_{-\infty}^{\infty} d\tau\ f(\mathbf{k},\mathbf{Q};\tau)G^{(0)}_{A\ B}(\mathbf{k},\tau)\check{G}_{A\dagger A}(\mathbf{Q}-\mathbf{k},\mathbf{k}';t-\tau)$$

$$G_{B\dagger A}(\mathbf{k},\mathbf{k}';t) = \sum_{\mathbf{Q}}\int_{-\infty}^{\infty} d\tau\ f^{*}(\mathbf{k}',\mathbf{Q};\tau)\hat{G}_{A\dagger A}(\mathbf{k},\mathbf{k}'-\mathbf{Q};\tau)G^{(0)}_{B\dagger A}(\mathbf{k};t-\tau)$$

$$\begin{aligned} G_{B\dagger B}(\mathbf{k},\mathbf{k}';t) = {} & G^{(0)}_{B\ B}(\mathbf{k};t)\delta_{\mathbf{k}\mathbf{k}'} + \sum_{\mathbf{Q}}\sum_{\mathbf{Q}'}\int_{-\infty}^{\infty}\int_{-\infty}^{\infty} d\tau_1 d\tau_2 \\ & \times f(\mathbf{k},\mathbf{Q};\tau_1)f^{*}(\mathbf{k}',\mathbf{Q}';\tau_2)G^{(0)}_{A\dagger B}(\mathbf{k};\tau_1) \\ & \times G_{A\dagger A}(\mathbf{k}-\mathbf{Q},\mathbf{k}'-\mathbf{Q}';\tau_1-\tau_2)G^{(0)}_{B\dagger A}(\mathbf{k}';\tau_2)\ , \end{aligned} \tag{A.4}$$

with $G^{(0)}_{A\dagger B}(\mathbf{k};t) \equiv -i\langle 0|T\{A^{\dagger}(t)B\}|0\rangle$

and $G^{(0)}_{B\dagger A}(\mathbf{k};t) \equiv -i\langle 0|T\{B^{\dagger}(t)A\}|0\rangle$.

Let $G^{(1)}_{A\dagger A}(\mathbf{k};t) \equiv G_{A\dagger A}(\mathbf{k},\mathbf{k};t)$,

and $G^{(\infty)}_{B\dagger B}(\mathbf{Q};t) \equiv -i\langle 0|T\{B^{\dagger}_{\mathbf{Q}}(t)B_{\mathbf{Q}}S(\infty)\}|0\rangle$,

then the emission rate $W_{\mathbf{k}}$, which includes any order of multi-polariton scattering process, is given from eq.(2.15);

$$\begin{aligned} W_{\mathbf{k}} = {} & G^{(1)}_{A\dagger A}(\mathbf{k};0-)\int_{-\infty}^{\infty} d\tau\Big(1+\sum_{\mathbf{Q}}|g(\mathbf{k},\mathbf{Q}-\mathbf{k})|^{2}G^{(\infty)}_{B\dagger B}(\mathbf{Q},\tau)\Big) \\ & \times G^{(1)}_{A\dagger A}(\mathbf{Q}-\mathbf{k};-0-\tau)G^{(1)}_{A\dagger A}(\mathbf{k};+0-\tau). \end{aligned}$$

The corresponding diagram is shown in Fig.A-2.

Here, we neglect another type of diagrams because their contribution to $W_{\mathbf{k}}$ is very small, as is proved by the perturbational expansion of the interaction V_3.

The excitonic molecule Green's function $G^{(\infty)}_{B\dagger B}(\mathbf{Q},\tau)$ is obtained by means of the usual diagramatic methods for three

particle interactions, where the Green's functions $G_{A^\dagger A}(\mathbf{k},\mathbf{k}';t)$, $G_{A^\dagger B}(\mathbf{k},\mathbf{k}';t)$, $G_{B^\dagger A}(\mathbf{k},\mathbf{k}';t)$ and $G_{B^\dagger B}(\mathbf{k},\mathbf{k}';t)$ are used as 0-th order Green's functions. Thus, $G^{(\infty)}_{B^\dagger B}(\mathbf{Q},\tau)$ is expressed as a solution of complicated simultaneous integral equations which are omitted here.

§ Appendix B

In this appendix, we derive the boundary conditions of eqs.(3.3).

The forward propagating waves are α_F, β_{F1} and β_{B2}. They are coupled with one another and compose three eigen modes.

Their eigen frequencies and relative amplitudes are determined by the following equation:

$$\begin{pmatrix} \omega-\omega_p(k), & -2, & -2 \\ -G^2(|\alpha_F|^2-2N_F), & \omega-\omega_m(2k)+\omega_p(k), & 0 \\ -G^2(|\alpha_F|^2-2N_0), & 0, & \omega-\omega_m(2k)+\omega_p(k) \end{pmatrix} \begin{pmatrix} \alpha_F \\ G\beta_{F1} \\ G\beta_{B2} \end{pmatrix} = \begin{pmatrix} 0 \\ 0 \\ 0 \end{pmatrix} \tag{B.1}$$

or the eigen value equation:

$$(\omega-\omega_p(k))(\omega-\omega_m(2k)+\omega_p(k)) - 2G^2(|\alpha_F|^2-2N_F)(\omega-\omega_m(2k)+\omega_p(k)) - 2G^2(|\alpha_F|^2-2N_0)(\omega-\omega_m(2k)+\omega_p(k))=0. \tag{B.2}$$

Under the off-resonant excitation on the lower energy side, only the lowest eigen mode is excited. Thus, the boundary conditions are decided as:

$$\begin{aligned} \alpha_F(0,\tau) &= tE_I'(\tau) + \gamma e^{i\delta}\alpha_B(0,\tau-2\Delta\tau) , \\ \alpha_B(\Delta\tau,\tau) &= \gamma\alpha_F(\Delta\tau,\tau) , \\ \beta_{F1}(\Delta\tau,\tau) &= \gamma e^{i\delta}\beta_{B1}(0,\tau-2\Delta\tau) + t\,C_1\,E_I'(\tau) , \\ \beta_{B1}(\Delta\tau,\tau) &= \gamma\beta_{F1}(\Delta\tau,\tau) , \\ \beta_{F2}(0,\tau) &= \gamma e^{-i\delta}\beta_{F2}(0,\tau-2\Delta\tau) + t\,C_2\,E_I'(\tau) , \\ \beta_{F2}(\Delta\tau,\tau) &= \gamma\beta_{B2}(\Delta\tau,\tau) , \end{aligned} \tag{B.3}$$

where

$$C_1 = \frac{2G\{|\alpha_F|^2-2N_F\}}{(2\omega_p-\omega_m)+\sqrt{(\omega_m-2\omega_p)^2+8G^2(|\alpha_F|^2-N_F-N_0)}} \quad ,$$

$$C_2 = \frac{2G\{|\alpha_F|^2-2N_0\}}{(2\omega_p-\omega_m)+\sqrt{(\omega_m-2\omega_p)^2+8G^2(|\alpha_F|^2-N_F-N_0)}} \quad ,$$

$$E_I'(\tau) = \left[\frac{C}{4\pi h\omega_p v_g(1+|C_1|^2+|C_2|^2)}\right]^{1/2} \cdot E_I(\tau) \quad , \qquad \text{(B.4)}$$

C is the velocity of light in the vacuum and $E_I(\tau)$ is the amplitude of incident laser light.

References

1) E. Hanamura: Solid State Commun. 12, 951(1973).

2) G.M. Gale and A. Mysyrowicz: Phys. Rev. Lett. 32, 727(1974).

3) M. Kuwata, T. Mita and N. Nagasawa: J. Phys. Soc. Jpn. 50, 2467(1981).

4) T. Itoh, T. Katohno and M. Ueta: J. Phys. Soc. Jpn. 53, 844(1984).

5) E. Hanamura and T. Takagahara: J. Phys. Soc. Jpn. 47, 410(1979).

6) T. Itoh and T. Suzuki: J. Phys. Soc. Jpn. 45, 1939(1978).

7) N. Nagasawa, T. Mita and M. Ueta: J. Phys. Soc. Jpn. 41, 929(1976).

8) J.B. Grun, B. Hönerlage and R. Levy: Solid State Commun. 46, 51(1983).

9) T. Itoh, T. Katohno, T. Kirihara and M. Ueta: J. Phys. Soc. Jpn. 53, 854(1984).

10) T. Tokihiro and E. Hanamura: Solid State Commun. 52, 771 (1984).

11) C.M. Bouden, M. Ciftan and H.R. Robe (ed.): Optical Bistability, Plenum Press (1981).

12) C.M. Bouden, H.M. Gibbes and S.L. McCall (ed.): Optical Bistability II, Plenum Press (1983).

13) H.M. Gibbs, S.L. McCall and T.N.C. Venkatesan: Phys. Rev. Lett. 36, 1135(1976).

14) S.D. Smith and D.A.B. Miller: Proceedings of Intern. Conf. on Phys. Semiconductors, p.597(1981).

15) E. Hanamura: Solid State Commun. 37, 984(1981).

16) S.W. Koch and H. Haug: Phys. Rev. Lett. 46, 450(1981).

17) D. Sarid, N. Peyghambrian and M. Gibbs: Phys. Rev. B28, 1184(1983).

18) C.C. Sung and C.M. Bowden:Phys. Rev. A29, 1957(1984).

19) N. Peyghambarian, H.M. Gibbs, M.C. Rushford and D.A. Weinberger: Phys. Rev. Lett. 51, 1692(1983).

20) B. Honerlage, J.Y. Bigot and R. Levi: in Proceedings of Optical Bistability Conference, Rochester (1983) in Ref.[12].

21) J.J. Hopfield: Phys. Rev. 112, 1555(1958), J. Phys. Soc. Jpn. 21, Suppl. 77(1966).

22) T. Itoh, S. Watanabe and M. Ueta: J. Phys. Soc. Jpn. 48, 542(1980).

23) R.J. Glauber: Phys. Rev. 131, 2766(1963).

24) S.T. Belyaev: Soviet Phys. JETP 7, 289(1958).

25) N.N. Bogolyubov: Soviet Phys. JETP 7, 41(1958).

26) H.M. Gibbs, S.S. Tarng, J.L. Jewell, D.A. Weinberger, K. Tai, A.C. Gossard, S.L. McCall, A. Passner and W. Wiegmann: Appl. Phys. Lett. 41, 221(1982).

27) S.I. Pekar: Crystal Optics and Additional Light Waves, Benjamin (1983).

28) F. Urbach: Phys. Rev. 92, 1324(1953).

29) W. Martienssen: J. Phys. Chem. Solids 2, 257(1957).

30) K. Ikeda: Optics Commun. 30, 257(1979).

31) J.L. Jewell, H.M. Gibbs, S.S.Jarng, A.C. Gossard and W. Wiegmann: Appl. Phys. Lett. 40, 291(1982).

32) P. Nozieres and C.T. de Dominicis: Phys. Rev. 178, 1097 (1969).

Figure Captions

Fig.1. Diagram contributing to (a) the Raman scattering with the coherent external lines F_0 and (b) the luminescence with the external lines F_Q.

Fig.2. (a) Diagram inducing the X_T- and X_L-bands when the external lines are F_0. (b) Diagram inducing the L_T- and L_L-bands when the external lines are F_Q.

Fig.3. Peak frequencies of the emission spectra as a function of the incident laser frequency ω_0. Open and closed circles denote the observations[4] and the solid lines are calculated in this thesis with the material constants for CuCl[4]. The dotted lines and the broken lines show, respectively, the M^R-bands and the calculated X_T-bands for the forward scattering configulation.

Fig.4. The physical meanings of field operators (eqs.(3.2)).

Fig.5. Typical off-resonance(Δ) dependence of input-output hysteresis curve. Curves (a), (b) and (c) are for Δ=0.9meV, 1.2meV and 1.5meV, respectively, where ℓ=5.0μm and δ=0.3.

Fig.6. Typical detuning(δ) dependence of input-output hysteresis curve. Curves (a), (b) and (c) are for δ=-0.1, -0.2 and -0.3 respectively, where ℓ=5.0μm and Δ=1.5meV.

Fig.7. Off-resonance(Δ) and sample-length(ℓ) dependence of the holding power in coherent optical bistability.

Fig.8. A figure similar to Fig.7 in incoherent optical bistability.

Fig.9. Off-resonance(Δ) dependence of holding power. Curves (a) and (b) are for incoherent optical bistability and for coherent

optical bistability.

Fig.10. Sample length (ℓ) dependence of holding power. Curves (a) and (b) are similar to Fig.9.

Fig.11. Transient response of coherent optical bistability. Transmitted power (curve(b)) switches from off-state to on-state with respect to the change of incident power (curve(a)).

Fig.12. A figure similar to Fig.11. This case shows switch-off behaviour.

Fig.A-1. The diagrams correspondig to eqs. (A.2)-(A.3b).

Fig.A-2. The diagram of the emission rate W_k.

Table 1

$\gamma_{\parallel} = 2.2\times10^{-3}$meV, $\Gamma = 2.2\times10^{-2}$meV

$|G|^2 = 5.5\times10^{-18}(\text{meV})^2\text{cm}^3$, $A = 3.5\times10^{10}\text{meV/KW}^2$

$\gamma' = 4.4\times10^{-4}$meV/KW

$v_g = 3.6\times10^{8}$cm/s

$R = 0.9$.

The other material constants are the same as those in Ref.[4].

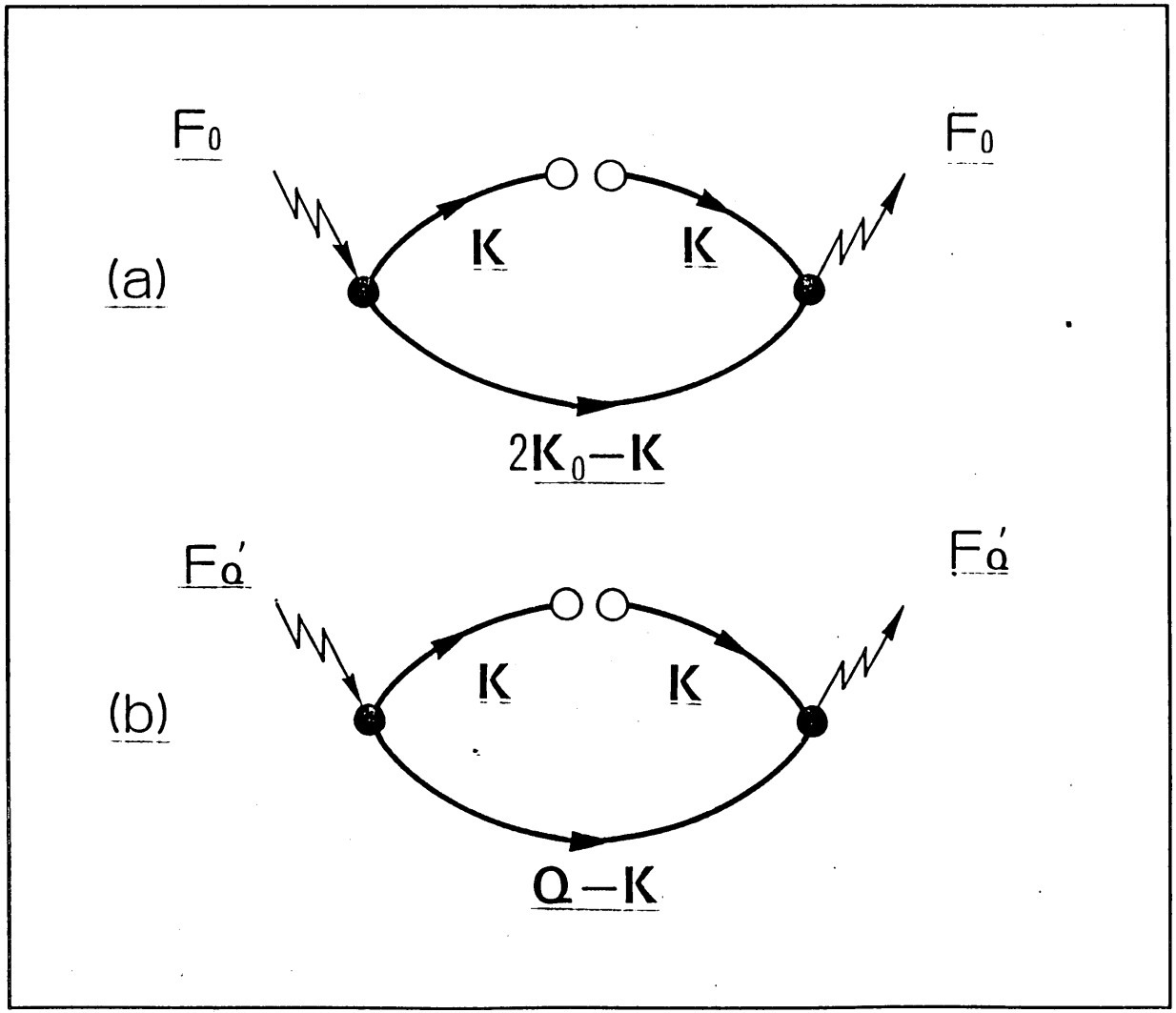

Fig. 1

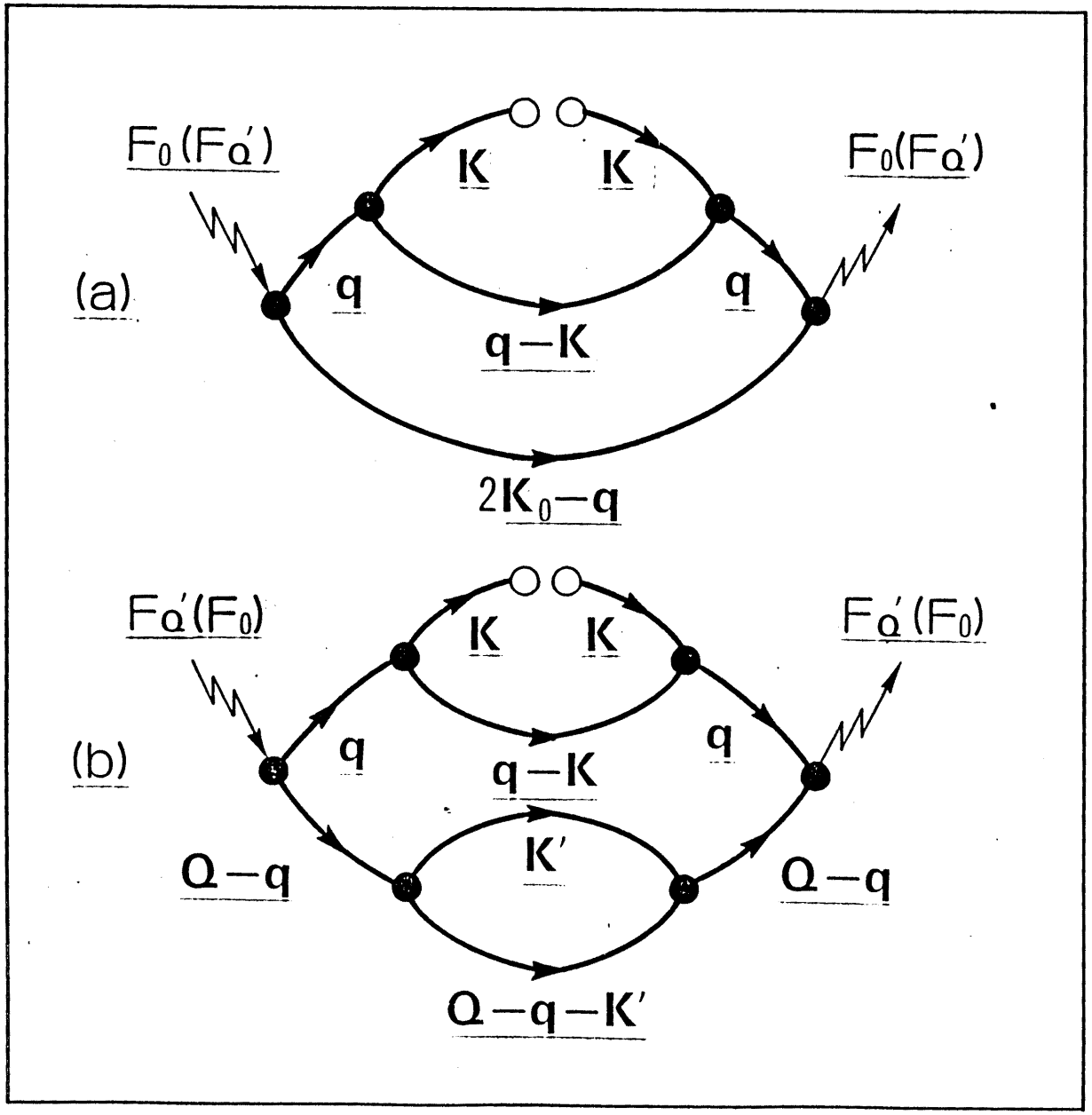

Fig.2

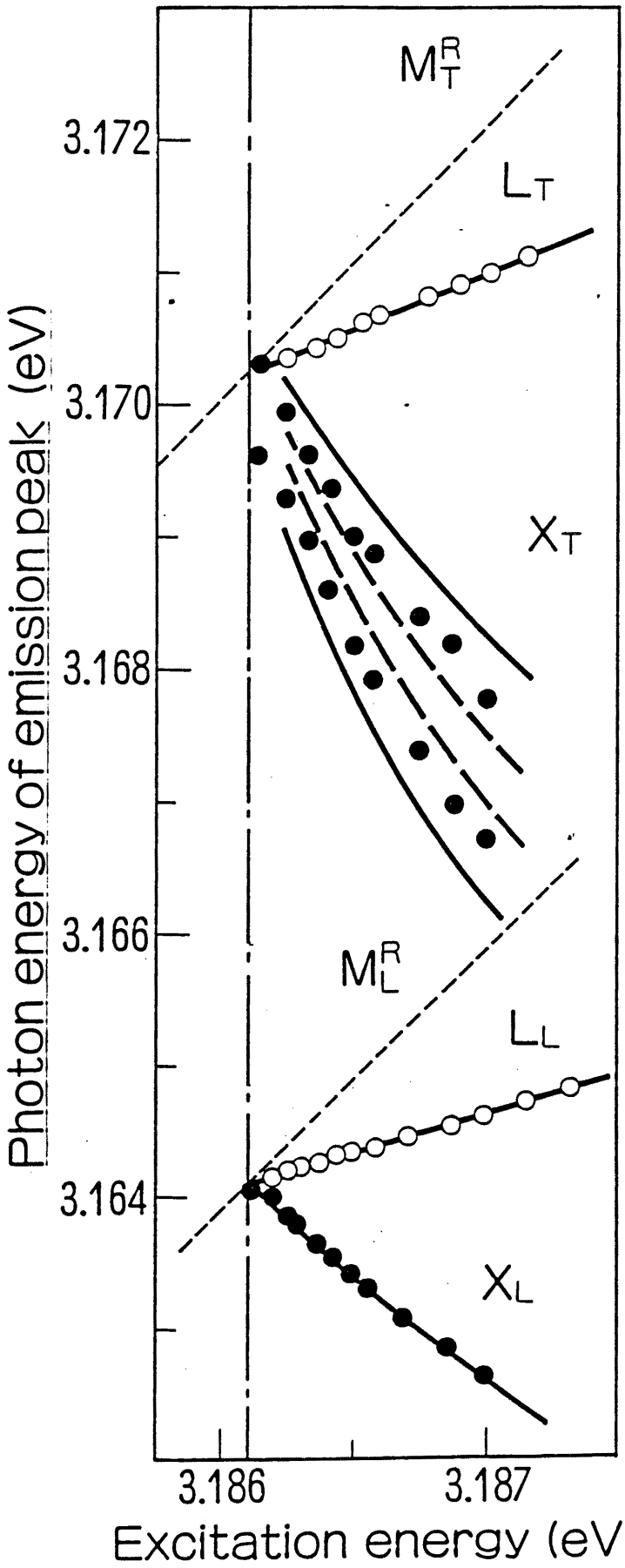
M_T^R
L_T
X_T
M_L^R
L_L
X_L
3.172
3.170
3.168
3.166
3.164
3.186
3.187
Photon energy of emission peak (eV)
Excitation energy (eV)

Fig.3

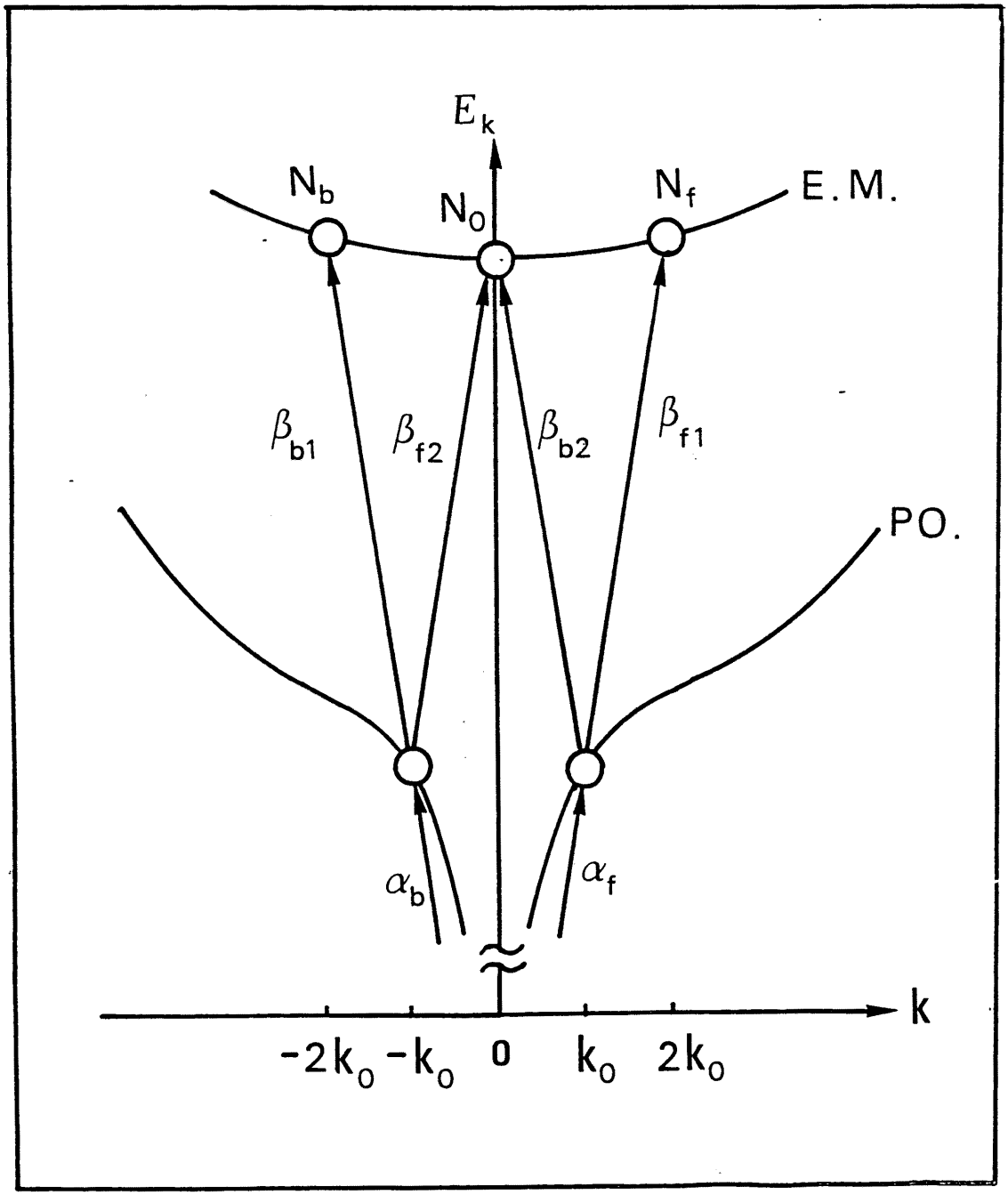
E_k
N_b
N_0
N_f
E.M.
β_{b1}
β_{f2}
β_{b2}
β_{f1}
PO.
α_b
α_f
k
$-2k_0$ $-k_0$ 0 k_0 $2k_0$

Fig.4

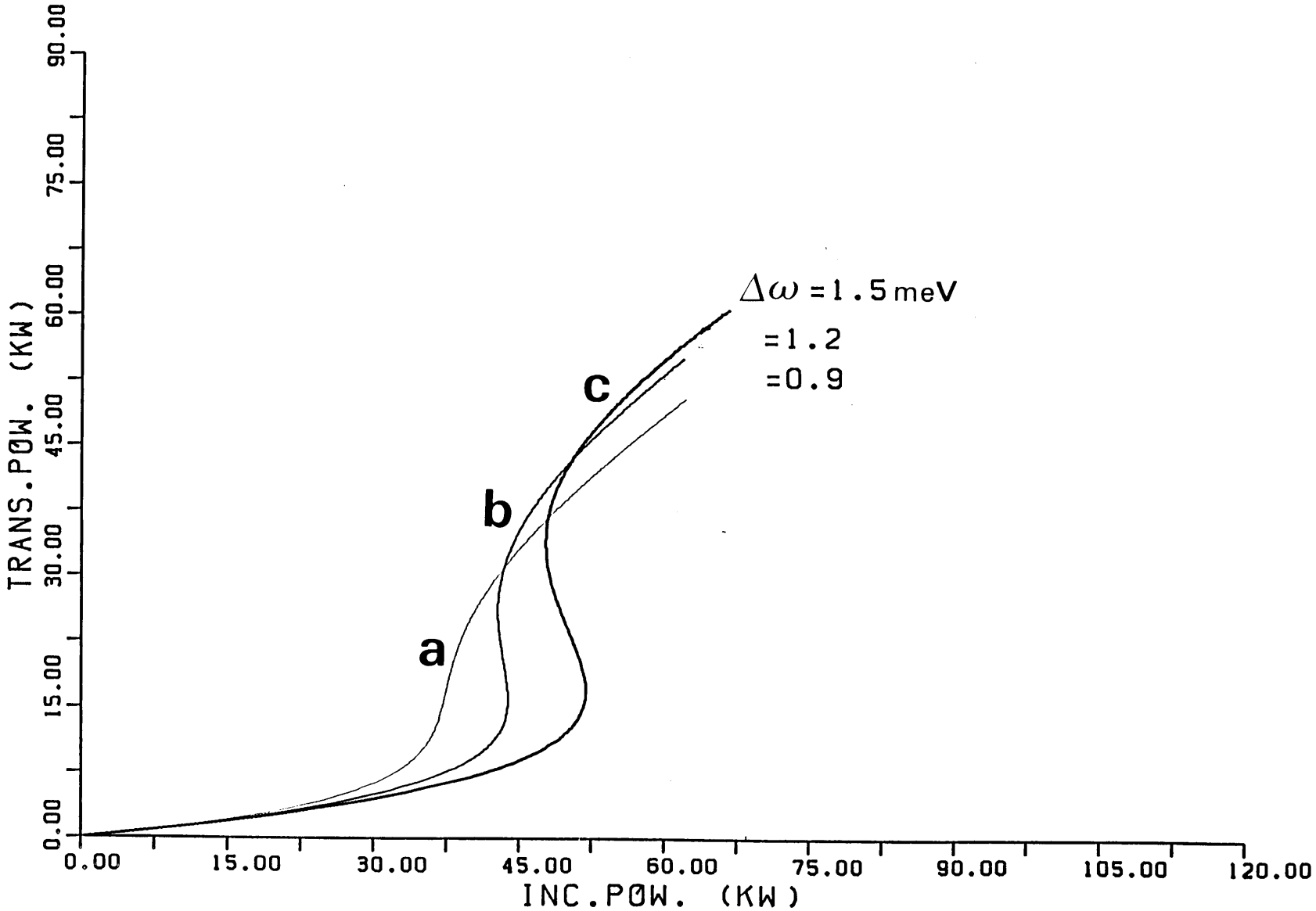
TRANS.PØW. (KW)
0.00
15.00
30.00
45.00
60.00
75.00
90.00
INC.PØW. (KW)
0.00
15.00
30.00
45.00
60.00
75.00
90.00
105.00
120.00
Δω =1.5meV
=1.2
=0.9
a
b
c

Fig.5

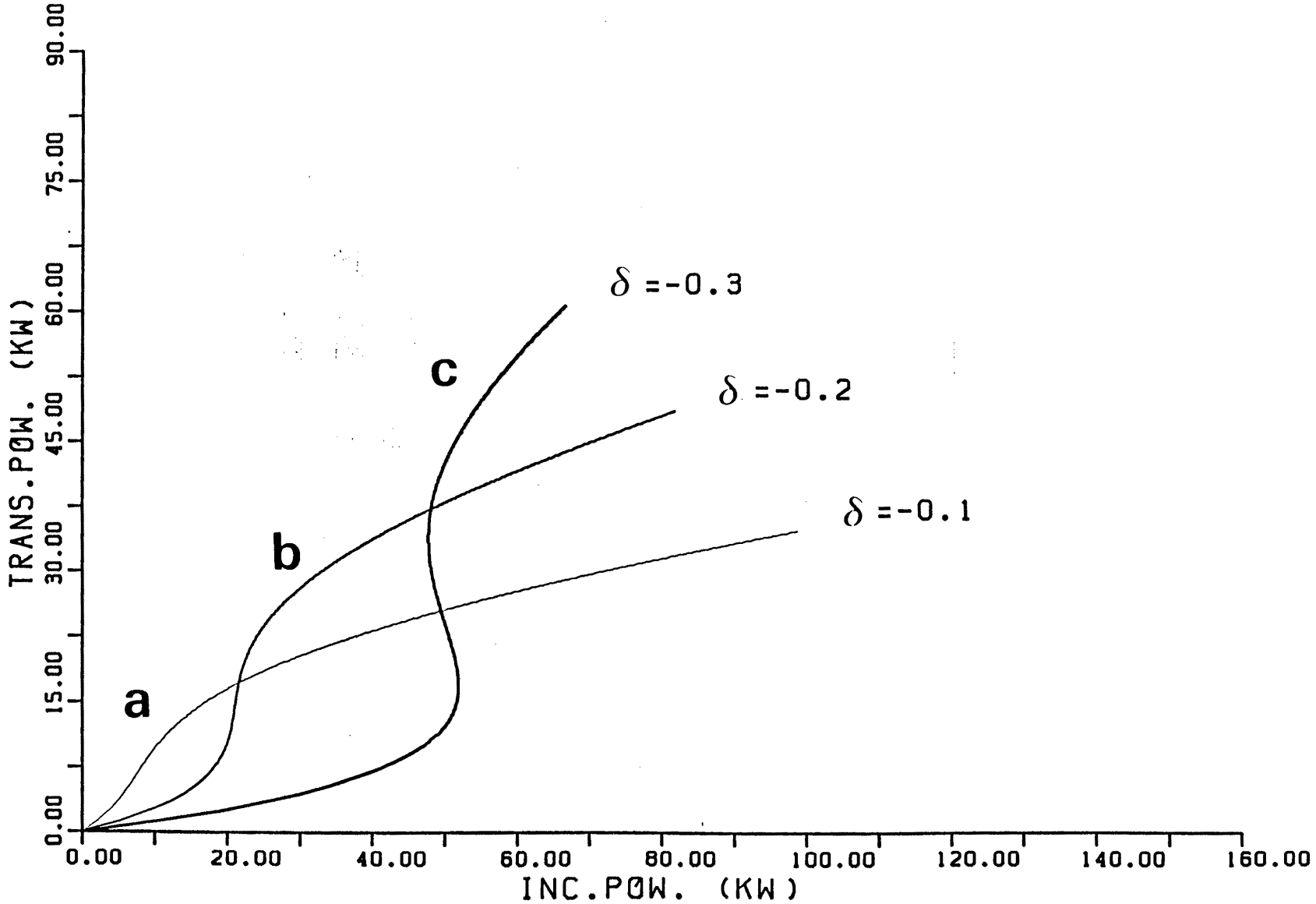
TRANS.PØW. (KW)
0.00
15.00
30.00
45.00
60.00
75.00
90.00
0.00
20.00
40.00
60.00
80.00
100.00
120.00
140.00
160.00
INC.PØW. (KW)
δ =-0.3
δ =-0.2
δ =-0.1
a
b
c

Fig.6

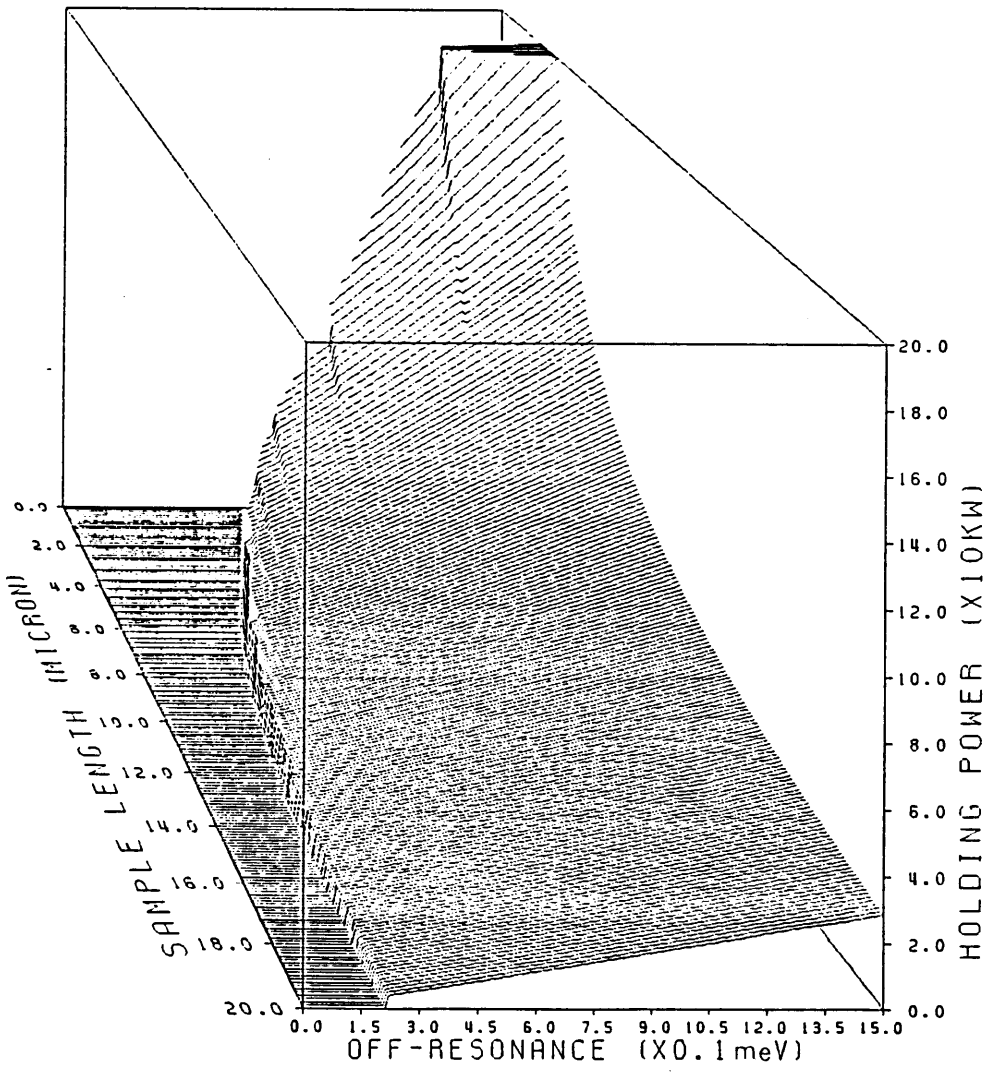
SAMPLE LENGTH (MICRON)
0.5
2.0
4.0
6.0
8.0
10.0
12.0
14.0
16.0
18.0
20.0
OFF-RESONANCE (X0.1meV)
0.0 1.5 3.0 4.5 6.0 7.5 9.0 10.5 12.0 13.5 15.0
HOLDING POWER (X10KW)
0.0
2.0
4.0
6.0
8.0
10.0
12.0
14.0
16.0
18.0
20.0

Fig.7

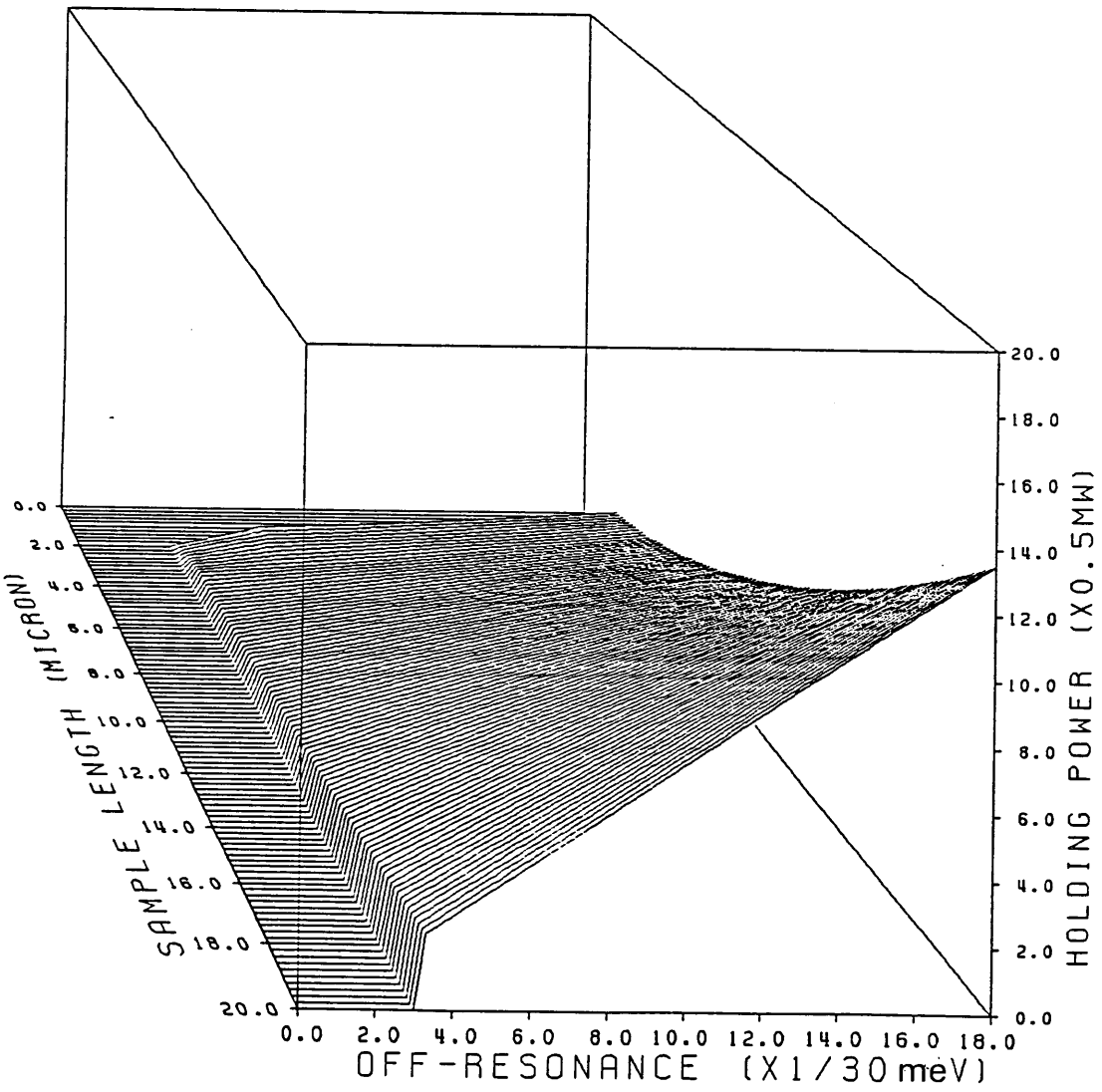
SAMPLE LENGTH (MICRON)
0.0
2.0
4.0
6.0
8.0
10.0
12.0
14.0
16.0
18.0
20.0
OFF-RESONANCE (X1/30meV)
0.0 2.0 4.0 6.0 8.0 10.0 12.0 14.0 16.0 18.0
HOLDING POWER (X0.5MW)
0.0
2.0
4.0
6.0
8.0
10.0
12.0
14.0
16.0
18.0
20.0

Fig.8

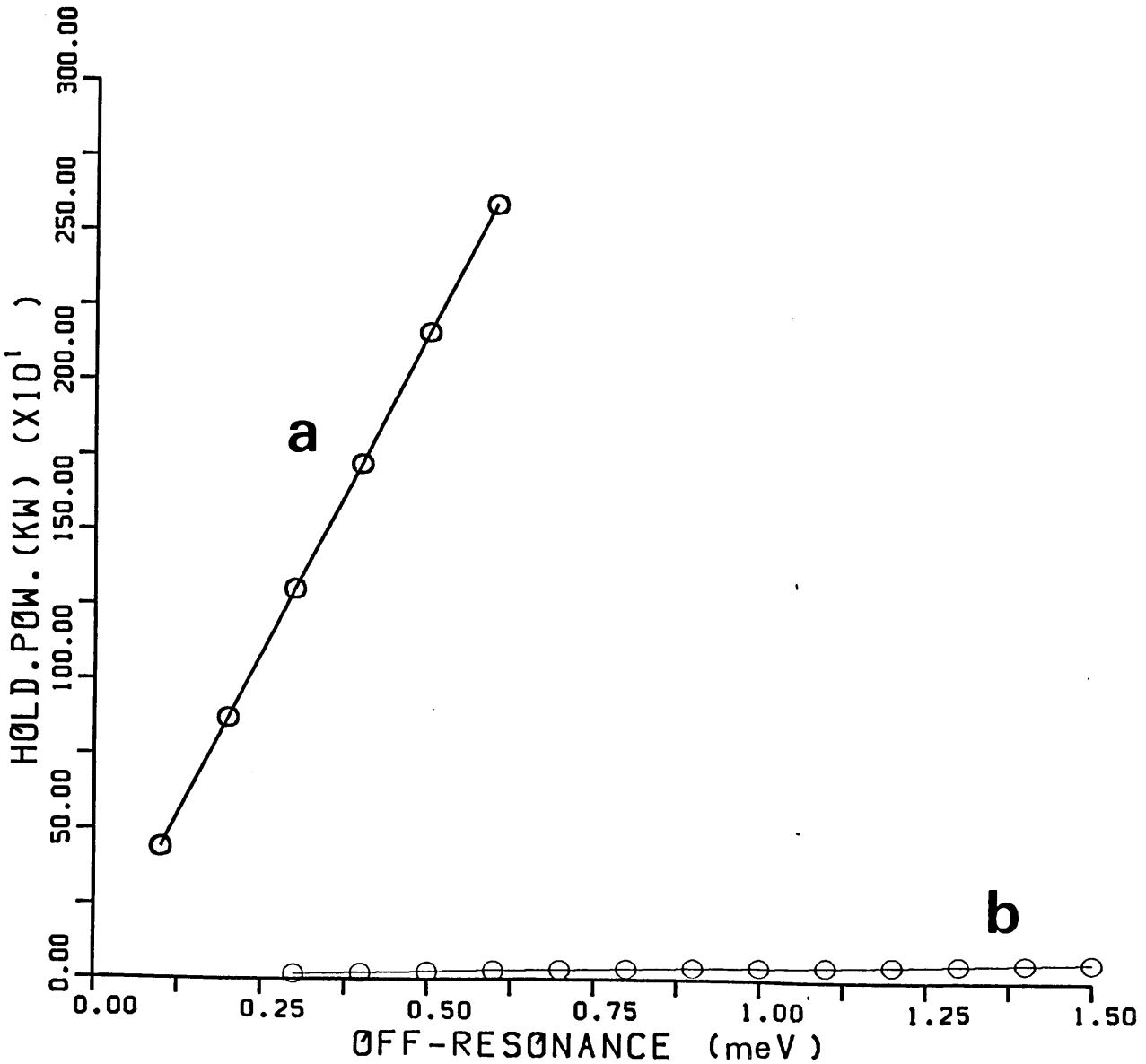
HØLD.PØW. (KW) (X10¹)
300.00
250.00
200.00
150.00
100.00
50.00
0.00
a
b
0.00
0.25
0.50
0.75
1.00
1.25
1.50
ØFF-RESØNANCE (meV)

Fig.9

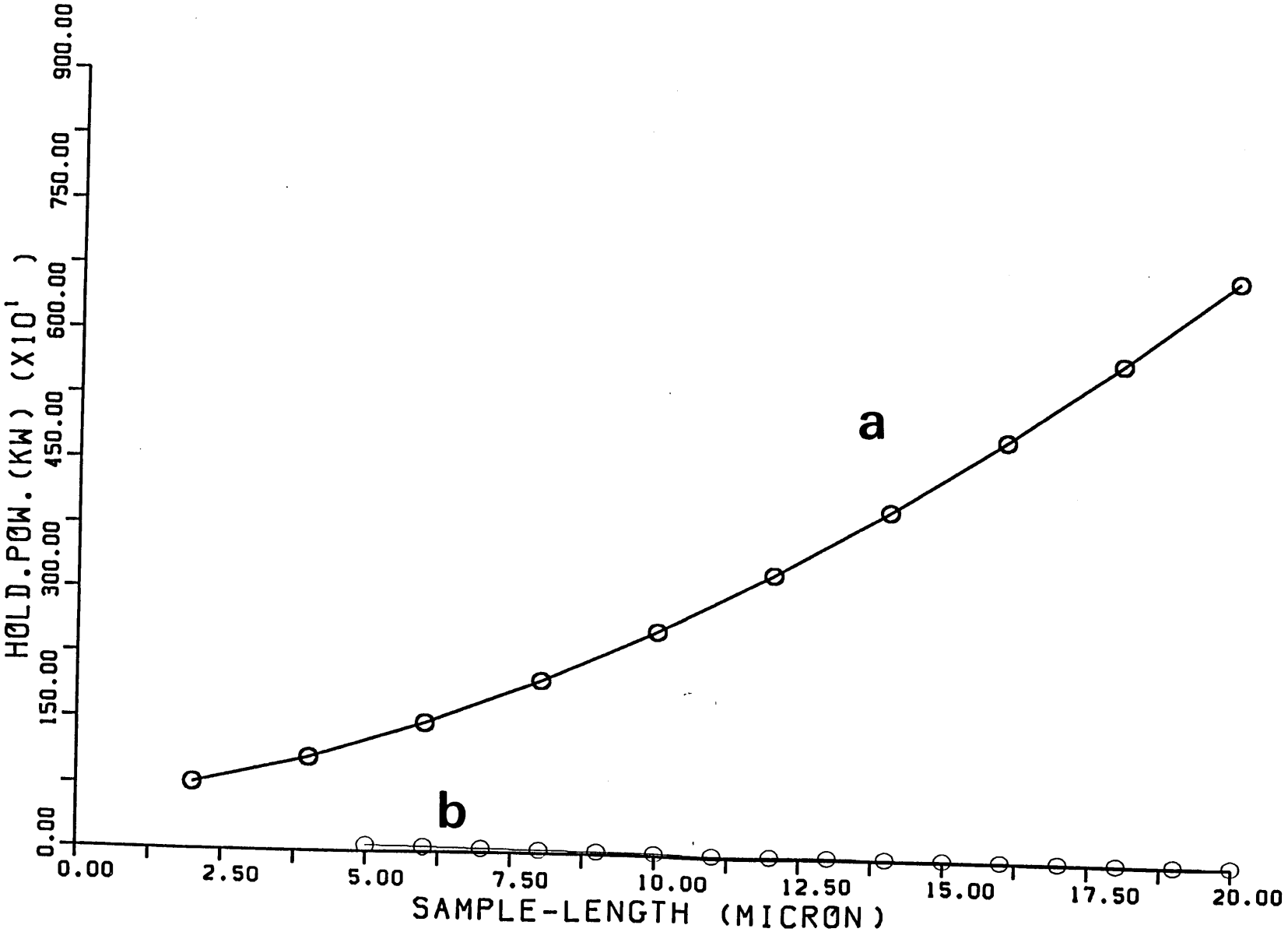
HOLD.POW. (KW) (X10¹)
900.00
750.00
600.00
450.00
300.00
150.00
0.00
a
b
0.00
2.50
5.00
7.50
10.00
12.50
15.00
17.50
20.00
SAMPLE-LENGTH (MICRON)

Fig.10

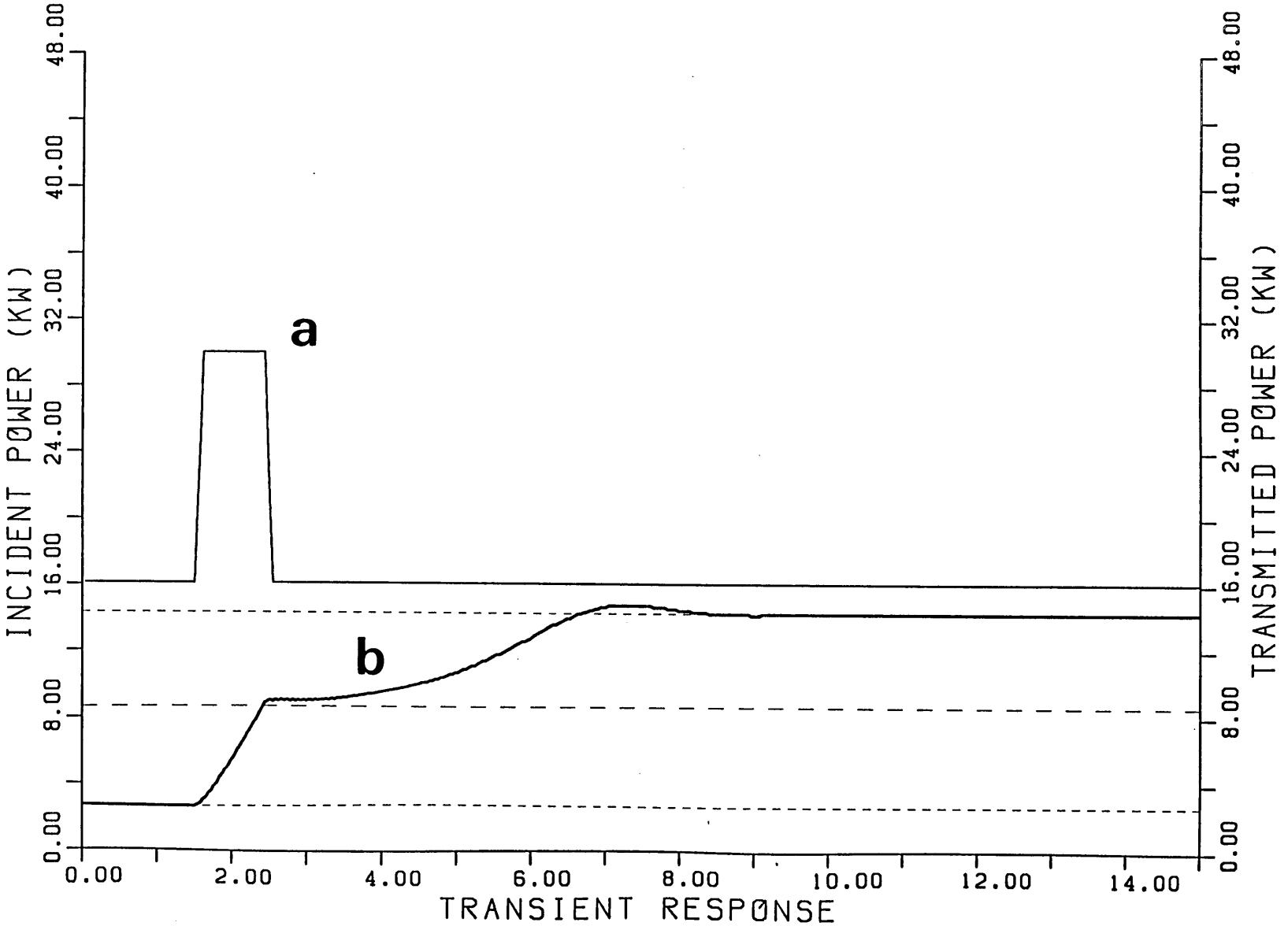
INCIDENT PØWER (KW)
TRANSMITTED PØWER (KW)
TRANSIENT RESPØNSE
a
b
0.00
8.00
16.00
24.00
32.00
40.00
48.00
0.00
2.00
4.00
6.00
8.00
10.00
12.00
14.00

Fig.11

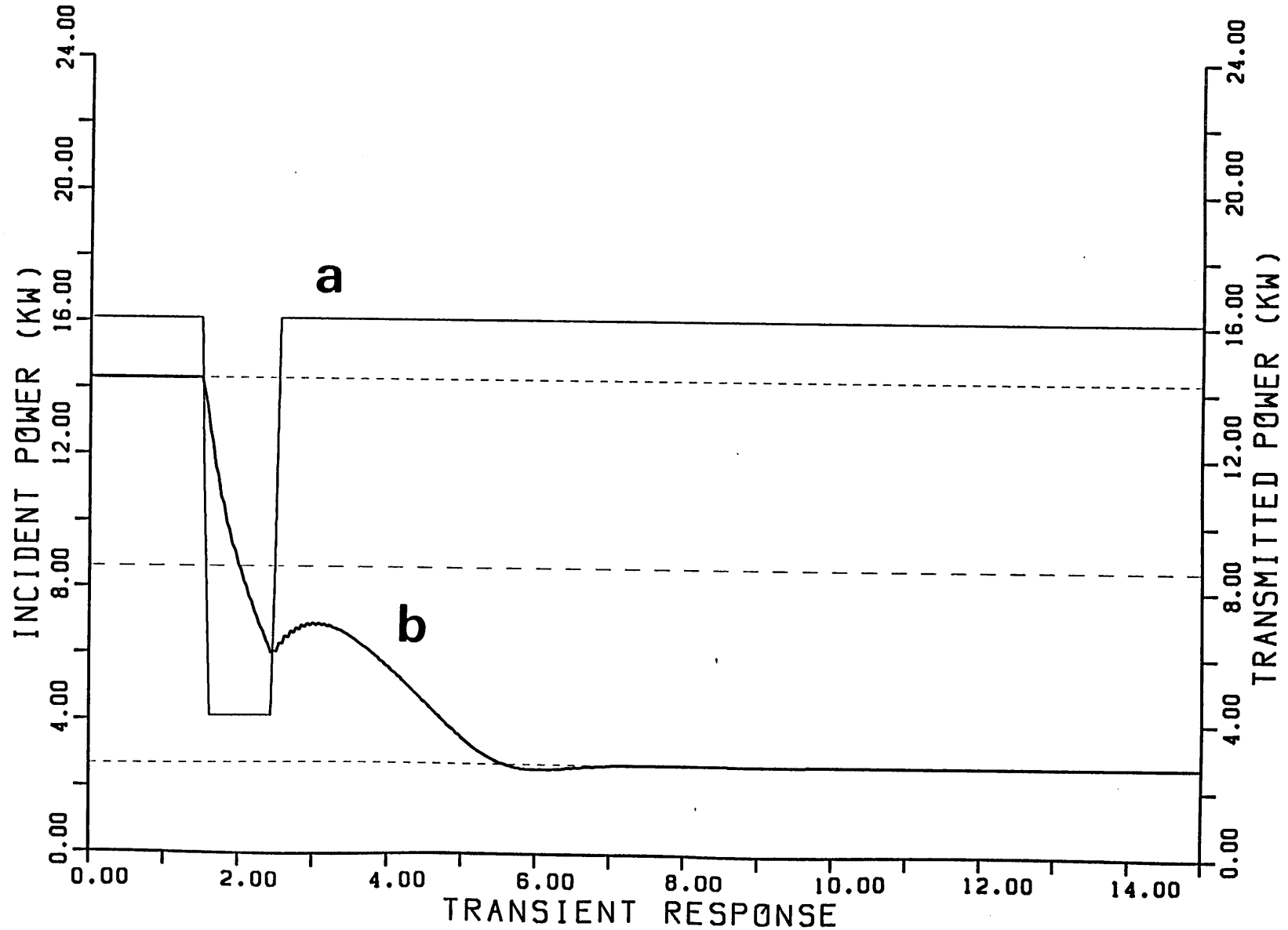
INCIDENT POWER (KW)
TRANSMITTED POWER (KW)
TRANSIENT RESPONSE
a
b
0.00
4.00
8.00
12.00
16.00
20.00
24.00
0.00
2.00
4.00
6.00
8.00
10.00
12.00
14.00

Fig.12

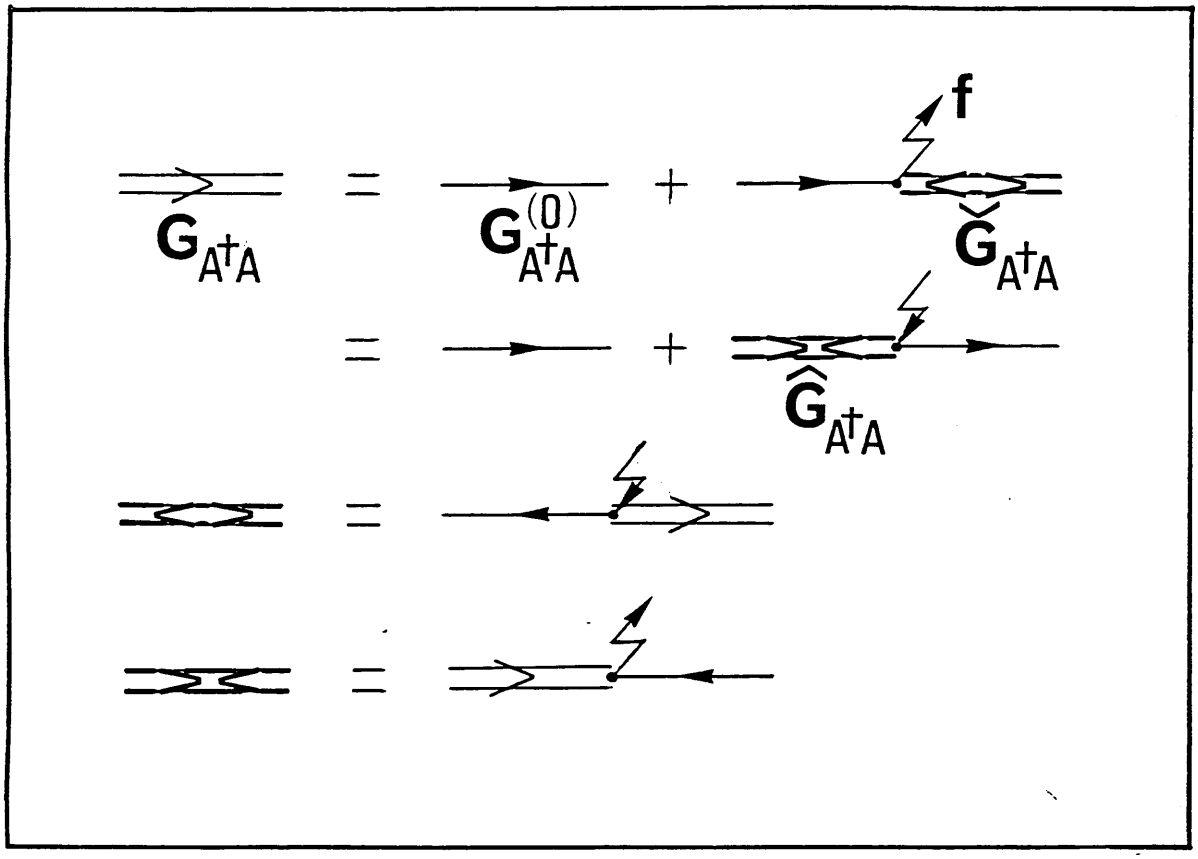
f
$G_{A^\dagger A}$
=
$G^{(0)}_{A^\dagger A}$
+
$\breve{G}_{A^\dagger A}$
=
+
$\hat{G}_{A^\dagger A}$
=
=

Fig.A-1

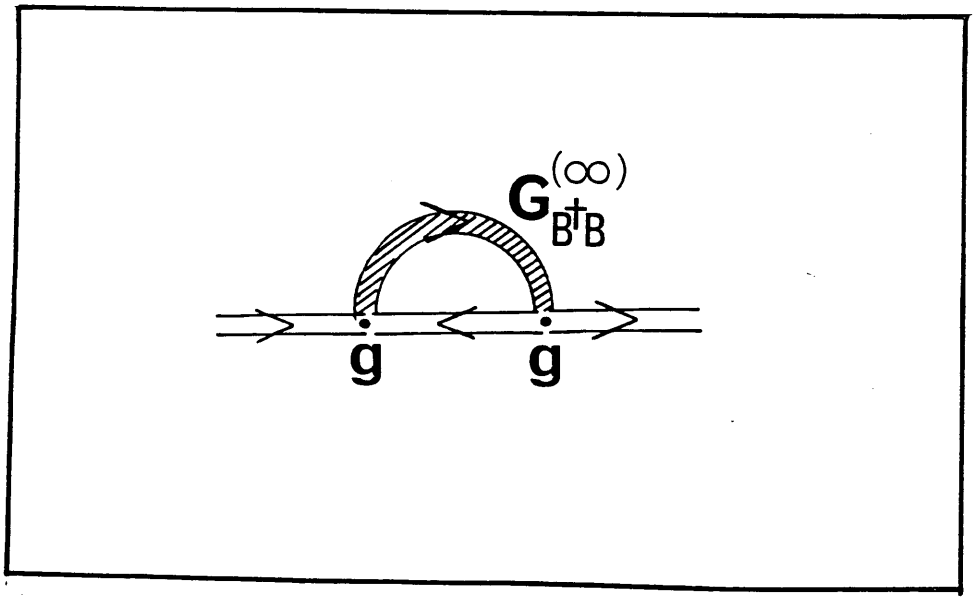
$G^{(\infty)}_{B^\dagger B}$
g
g

Fig.A-2